Glacier evolution in the South West slope of Nevado Coropuna

(Cordillera Ampato, Perú)

Néstor Campos Oset

Master Project

Master en Tecnologías de la Información Geográfica (TIG)

Universidad Complutense de Madrid

Director:

Prof. David Palacios (UCM)

Departamento de Análisis Geográfico Regional y Geografía Física

Grupo de Investigación en Geografía Física de Alta Montaña (GFAM)

ACKNOWLEDGEMENTS

I would like to gratefully and sincerely thank Dr. David Palacios for his help and guidance during the realization of this master thesis. I would also like to thank Dr. José Úbeda for his assistance and support. Thanks to GFAM-GEM for providing materials used for the analysis. And last but not least, a special thanks to my family, for their encouragement during this project and their unwavering support in all that I do.

TABLE OF CONTENTS

CHAPTER 1 INTRODUCTION 4

1.1 Geographic settings 4
1.2 Geologic settings 6
1.3 Climatic setting 8
1.4 Glacier hazards 10
1.5 Glacier evolution 11
1.6 Aims and objectives 15
1.7 Organization of the Thesis 15

CHAPTER 2 METHODOLOGY 16

2.1 Materials 16
2.2 Georeferencing 18
2.3 Moraine mapping 18
2.4 Glacier delimitation and surface calculation 20
2.5 ELAs AABR 22
2.5.1 ELAs AABR of 1955 and 2007 glaciers. 23
2.5.2 Paleo-ELAs AABR of paleo-glaciers. 27
2.6 Spatial model of ELAs and accumulation and ablation zones 28
2.6.1 ELAs spatial model 29
2.6.2 Accumulation and ablation zones spatial model 29
2.6.3 Surface calculation 30

CHAPTER 3 RESULTS 31

3.1. Moraine mapping 31
3.2 Glacier delimitation and surface calculation 32
3.3 ELAs ABBR 36
3.4 Spatial model of ELAs and accumulation and ablation zones 40

CHAPTER 4 DISCUSSION AND FUTURE WORK 45

4.1 Moraine mapping 45
4.2 Glacier delimitation and surface calculation 46
4.3 ELAs AABR 47
4.4 Conclusions 48

REFERENCES 49

TABLE OF FIGURES 55

CHAPTER 1

INTRODUCTION

Glaciers reveal clues about climate change, its ice make them valuable for climate research, also they are very important as a water supply for the population who is living around. Otherwise they can cause natural hazards like mudflows. The main aim of this project is to reconstruct the glacial phases in the SW slope of Nevado Coropuna in order to achieve valuable information of all the changes that have happened and analyze the glacier evolution.

1.1 Geographic settings

The Andes form an almost continuous topographic barrier along western South America (Anders et al., 2002) and pass through Peru and Bolivia, where they host the majority of the world's remaining tropical glaciers (Kaser and Osmaston, 2002). The Central Andes in South America are characterised by high altitudes, low temperatures, intensive insolation and extremely dry conditions. Quaternary landscapes are therefore often well preserved and are valuable archives for paleoenvironmental reconstruction. Moraines, for example, document former extensive glaciations even between 18 and 27º S – an area where today no glaciers exist despite altitudes above 6000 m, owing to the extreme aridity (Ammann et al., 2001). The Cordillera Ampato consists of three different mountain groups, Nevados Ampato, Coropuna, and Solimana, and lies in the Cordillera Occidental between lat 15º 24' and 15º51'S, and long 71º51' and 73º00'W. The range extends in an easterly direction for about 140 Km. The glacierized area, estimated from Landsat images, is 105 Km^2. The area lies entirely within the Pacific Ocean drainage and is drained by Rio de Majes and Rio Sihuas. The highest peak is the Nevado Coropuna at 6,426m asl.

Nevado Coropuna (6426 m; 15º 33'S, 72º 39'W), located 150km northwest of Arequipa, is both the highest peak in the Cordillera Ampato and the highest volcano in Peru. The mountain comprises four andesite domes separated by broad saddles and rises ~2000m above the surrounding puna on all but the south side. Here, incision of the underlying ignimbrite by the Rio Llacllaja, a tributary of the Colca Canyon, has resulted in relief of more than 3500 m. Although andesitic eruptions at Coropuna began during the late Miocene, the mountain's present structure is attributed to prolonged Quaternary volcanism (Venturelli et al., 1978; Weibel et al., 1978).

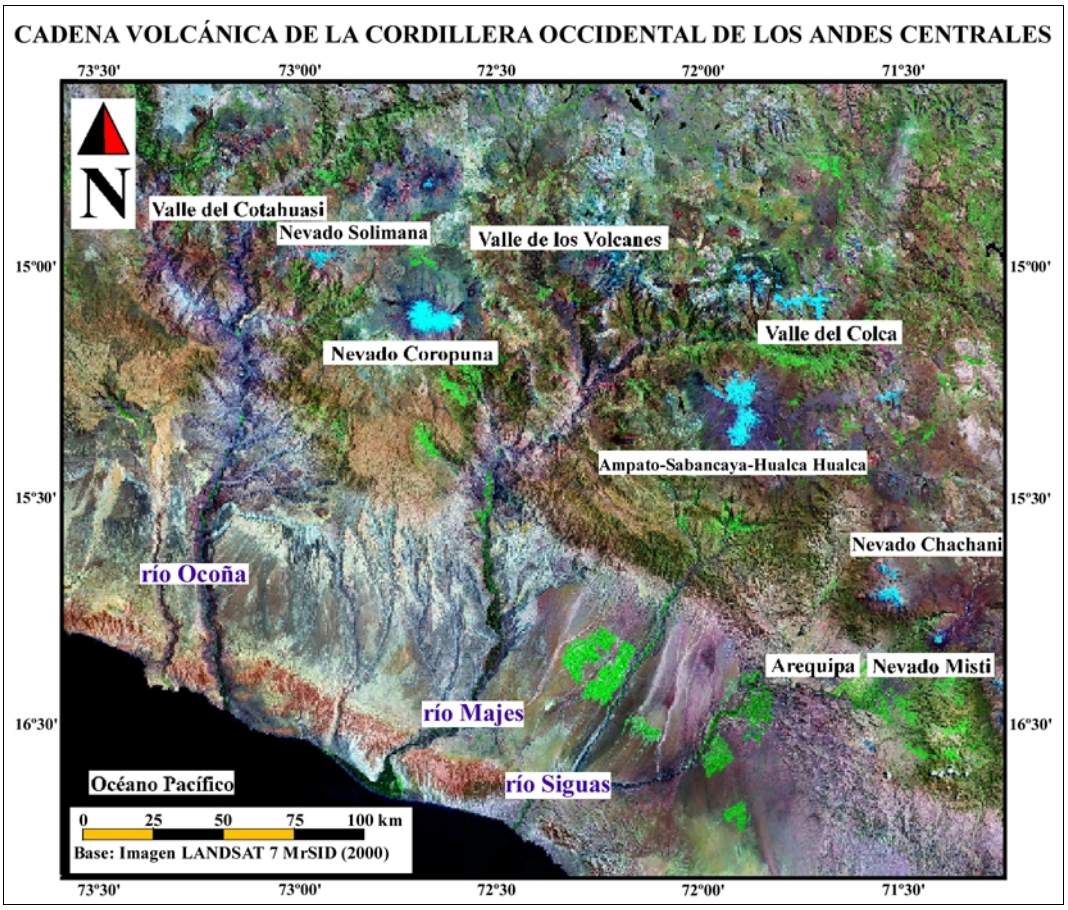

Figure 1. 1. Geographical setting or Cordillera Occidental. Landsat 7 MRSID (2000) image (GFAM-GEM).

According to the Peruvian Glacier Inventory (in 1998), the Cordillera Ampato has 93 tropical glaciers covering a total area of 147 Km^2, with an estimated volume of 5,12 Km^3. The tropical glaciers located on low-latitude, high-altitude mountain ranges are highly sensitive components of the environment and appear to react more immediately to fluctuations in climate than glaciers in the mid- and high-latitudes (Guilderson et al., 1994; Hostetler and Mix, 1999; Hostetler and Clark, 2000; Seltzer et al., 2002). In cross-section, the Andes consist of five topographic sections (west to east): the western slope, the Western Cordillera, the high-elevation Central Andean Plateau, the Eastern Cordillera, and the Subandean Zone (Isacks, 1988; Dewey and Lamb, 1992; Gubbels et al., 1993). The Central Andean Plateau, an internally drained region with a relatively constant altitude (~3500–4000m above sea level (a.s.l.)), lies between the Western and Eastern Cordillera and stretches from about 11º S to 27º S (Isacks, 1988; Kennan, 2000). The Central Andean Plateau is widest (up to about 500 km) between about 15º S and 25º S in the Central Andes, where it is known as the Altiplano in Peru and Bolivia and the Puna in Argentina (Dewey and Lamb, 1992).

From a glaciological point of view, the following delimitations give a useful definition of the Tropics (Kaser, 1995, 1998; Kaser et al., 1996).: they must be within (1) the astronomical tropics (radiative delimitation); (2) the area where the daily temperature variation exceeds the annual temperature variation (thermal delimitation) and (3) the oscillation area of the Inter Tropical Convergence Zone (ITCZ) (hygric delimitation).

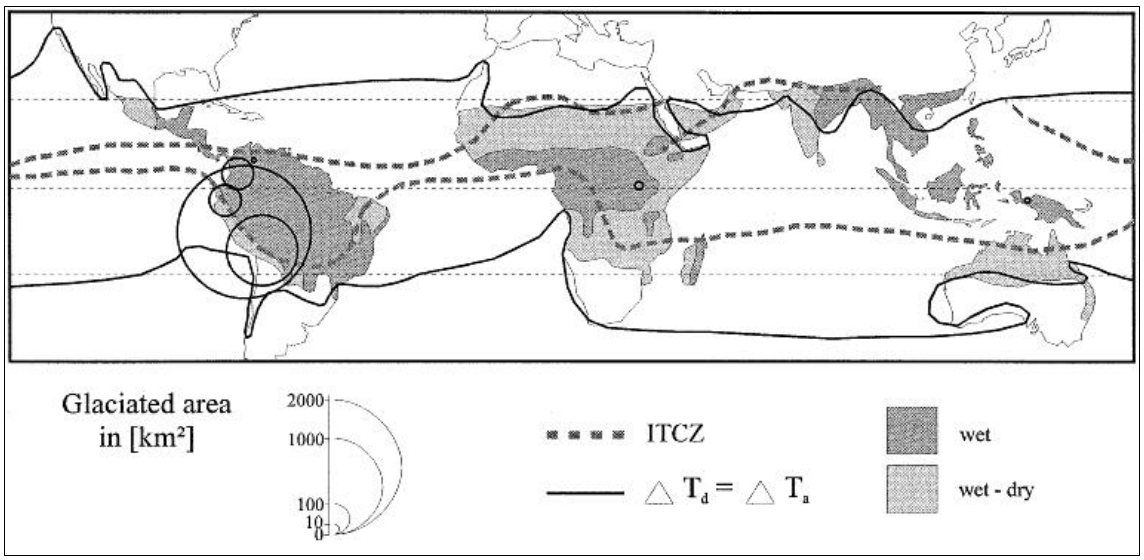

Figure 1. 2. The tropics and their delimitations from a glaciological point of view, and the distribution of glacier areas according to countries' ITCZ, taken directly from kaser (1999)

1.2 Geologic settings

The Andes vary considerably in structure, composition, volcanic activity and glacial history along their 9000km length. They have developed as oceanic lithosphere underlying the eastern Pacific Ocean has been subducted beneath continental ithosphere of the South American Plate (e.g. Jordan et al., 1983). The Andes consist of a variety of sedimentary, metasedimentary, plutonic and extrusive rocks ranging in age from Precambrian to Recent (Clapperton, 1993; Kley, 1999).

In the Central Andean region, glaciers dynamically couple atmospheric and tectonic processes through erosion. Located along a convergent plate boundary, the Andes have formed during the relatively continuous subduction of the oceanic Nazca plate beneath the South American continental plate since the Mesozoic (Allmendinger et al., 1997). The hypsometry, cross-range asymmetry, width, and maximum elevation of the Central Andes display a direct correspondence between climate zones and morphology (Montgomery et al., 2001). According to Bromley et al. (2011) the Nevado Coropuna comprises four andesite domes separated by broad saddles and rises ~2000m above the surrounding puna on all but the south side. Here, incision of the underlying ignimbrite by the Rio Llacllaja, a tributary of the Colca Canyon, has resulted in relief of more than 3500 m. Although andesitic eruptions at Coropuna began during the late Miocene, the mountain's present structure is attributed to prolonged Quaternary volcanism (Venturelli et al., 1978; Weibel et al., 1978).

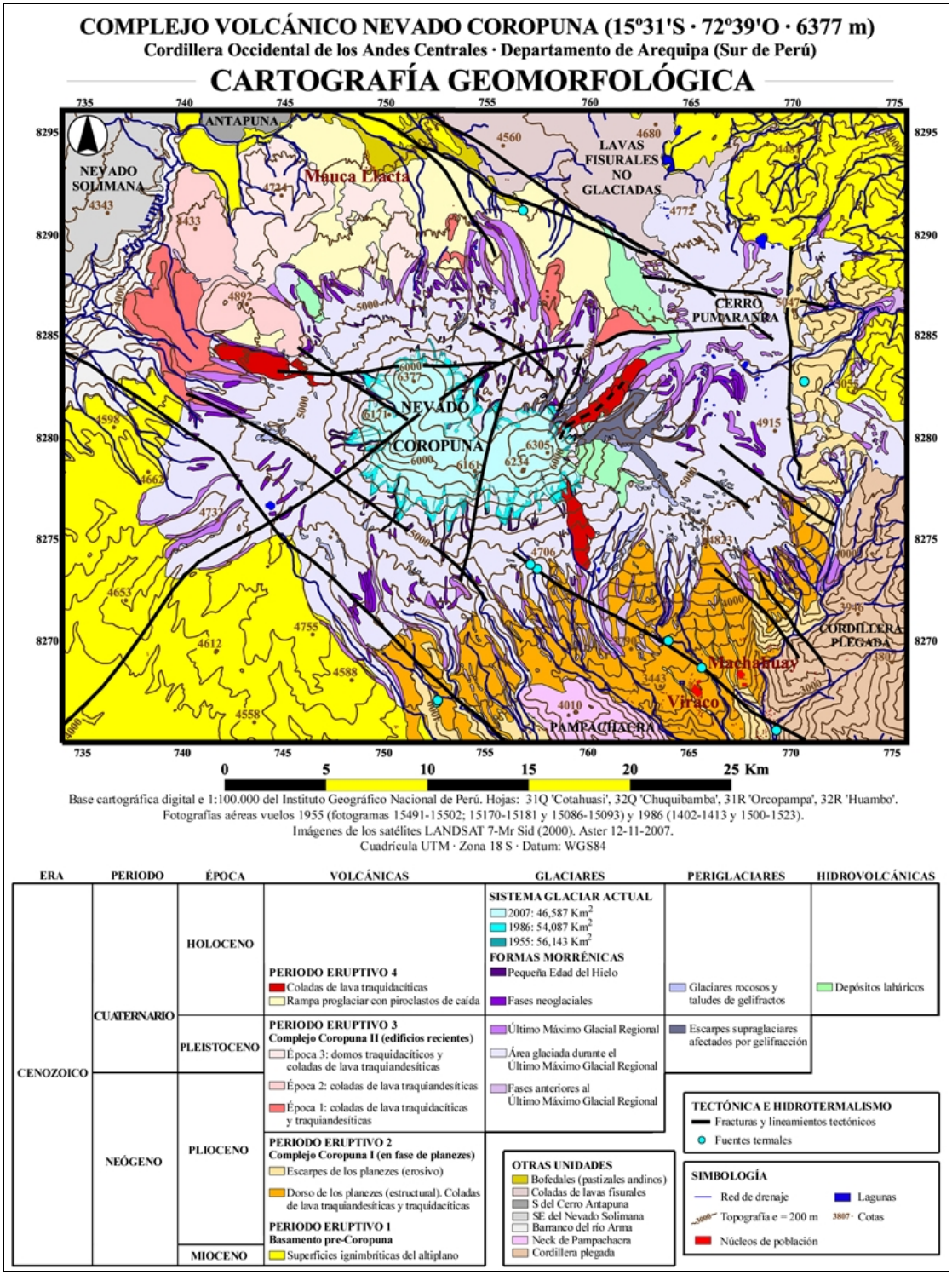

Figure 1. 3. Geomorphological cartography of Nevado Coropuna (GFAM-GEM).

1.3 Climatic setting

The main source of precipitation for the tropical Andes of the Southern Hemisphere lies to the east in the Atlantic Ocean and the Amazon Basin, and the primary transport mechanism is seasonal easterly winds (Johnson, 1976; Vuille and Keimig, 2004). The persistent inversion over the Pacific coast and strong Andean rain shadow effect combine to maintain a semi-arid climate at Coropuna. Most precipitation (~390mm water equivalent a^{-1} at 6080 m; Herreros et al., 2009) arrives during the brief summer wet season (December–March). Coropuna currently supports an ice cap (~60 km2; Racoviteanu et al., 2007) drained by 15 outlet glaciers, as well as extensive perennial snow. Due to aridity, glaciers are restricted to elevations significantly higher (5100–5500 m) than the local zero-degree isotherm (~4900 m; Dornbusch, 1998)

Within a perimeter of 60 km around the Nevado Coropuna, 15 meteorological stations (operated by the Peruvian SENAMHI, Servicio Nacional de Meteorologia e Hidrologia) provide important local climatic information. Monthly mean precipitation and air temperature are available from1964 to 2003. Data series from the four highest stations (Andagua: 3590 m; Arma: 4270 m; Orcopampa: 3780 m; Salamanca: 3200 m), panning 22 to 35 years, have been selected for a statistical study according to the consistency of the records. Seasonal temperature amplitudes are small. Contrastingly, seasonal precipitation amplitudes are very strong with most of the precipitation events taking place during the austral summer: 70 to 90% of the annual precipitation occurs from December to March (Fig. 2). A drastic decrease of precipitation was observed in 1982–1983 and 1992 during strong El Niño events (Fig. 2). It is worth noting that other notable El Niño episodes (such as in 1997) are not obvious in the precipitation records (Herreros, 2009).

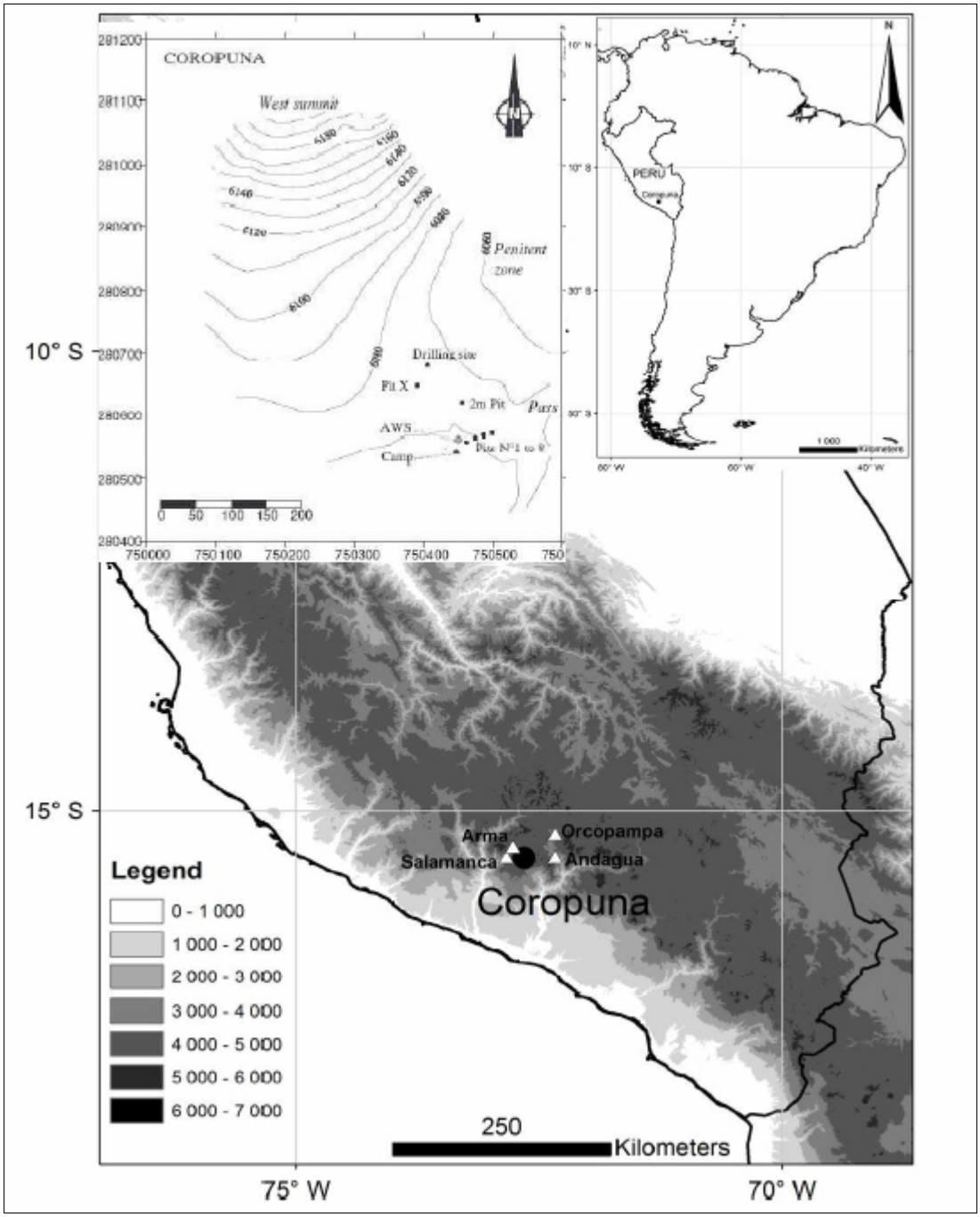

Figure 1. 4. Map of the Andes showing the location of the Nevado Coropuna and a schematic distribution of the weather stations located around (Salamanca, Arma, Orcopampa and Andagua). Taken directly from Herreros et al., (2009)

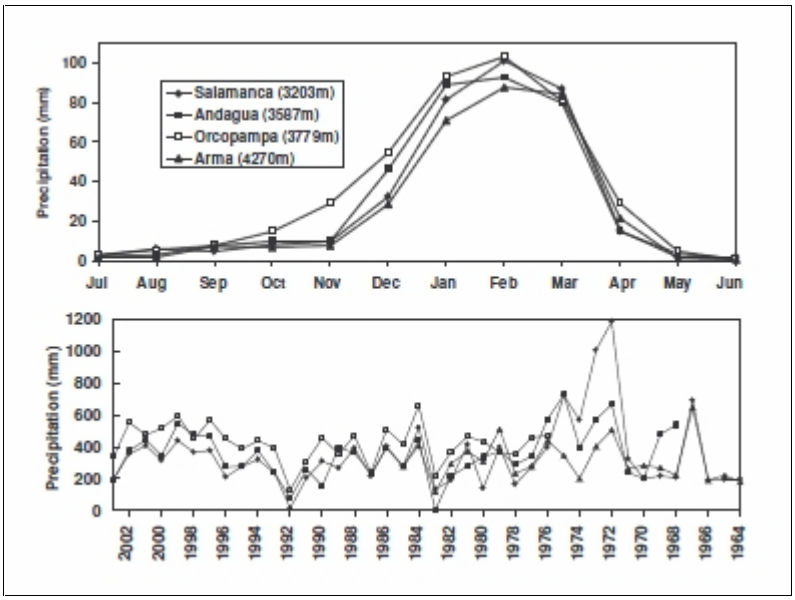

Figure 1. 5. Annual and monthly mean precipitation at selected SENAMHI-Peru stations: Salamanca (15_300 S, 72_500 W), Andagua (15_290 S, 72_200), Orcopampa (15_150, 72_200), Arma (15_240, 72_460) Herreros et al., (2009).

The tropical Andes of Peru have a wet season during the austral summer and a dry season during the austral winter (Johnson, 1976). During the wet season, prevailing easterlies deliver moisture from the Amazon lowlands, while the dry season is dominated by moisture-deficient westerlies from the Pacific Ocean (Garreaud et al., 2003). An east–west precipitation gradient across the Andes results, with more precipitation typically falling on the east-facing slopes of the eastern cordillera than on any of the slopes farther to the west (Kessler and Monheim, 1968; Johnson, 1976).

1.4 Glacier hazards

The current topographic context of the glaciers contribute to extreme natural hazards. Modern glaciers occupy steep slopes, causing concern for hazards in the form of ice fall and dangerous lake formations. The combination of active tectonic faulting, steep topography, and melting glaciers is tragic for human residents. Glacier-related hazards are common in high mountain regions. Climate change and intensification of human activities in mountains have attracted increasing interest to the related risks, where risk is understood as a function of hazard (probability) and damage potential (e.g., Fell 1994). The management of these risks is a complex task involving analysis, evaluation, and communication as well as prevention and mitigation (Greminger 2003).

Hazards associated with Andean volcanoes include pyroclastic and lava flows, lahars, debris flows generated by sector collapse, and tephra falls. More than 25,000 people have been killed by the >600 eruptions of these volcanoes catalogued since the year 1532, most of these by lahars generated during the eruption of Nevado del Ruiz, Colombia, in 1985, a clear indication that much more needs to be done concerning volcano hazard assessment and risk management in the Andes. Despite the fact that >20 million people live within < 100 km of an active Andean volcano, mostly in low-lying areas in the intermontane valleys of Colombia and Ecuador and the Central Valley of south-central Chile, only <25 of these volcanoes are continuously monitored for signs of activity (Stern, 2004). Coropuna has apparently not been active during since the

Late Glacial but three youthful lava flows, not dated yet, filled glacial-shaped valleys on the west, northeast and southeast flanks (Lamadon, 1999)

Lahar flows can be deadly because of their energy and speed. With the potential to flow at speeds up to 100 kilometres per hour (60 mph), and distances of more than 300 kilometres (190 mi), a lahar can cause catastrophic destruction in its path (Hoblitt et al., 1987). According with Tanguy et al. (1998) lahars have been responsible for 17% of volcano-related deaths between 1783 and 1997. Lahars have several possible causes: (1). Snow and glaciers can be melted by lava or pyroclastic flows during an eruption; (2). A flood caused by a glacier, lake breakout, or heavy rainfall can release a lahar; (3). Water from a crater lake, combined with volcanic material in an eruption.
Although lahars are typically associated with the effects of volcanic activity, lahars can occur even without any current volcanic activity, as long as the conditions are right to cause the collapse and movement of mud originating from existing volcanic ash deposits.(1). Snow and glaciers can melt during periods of mild weather; (2). Earthquakes underneath or close to the volcano can shake material loose and cause it to collapse triggering a lahar avalanche; (3). Rainfall or typhoons can cause the still-hanging slabs of solidified mud to come rushing down the causing devastating results. (USGS, 2000)

The recognition of the slopes of Nevado Coropuna has proved that lahars are relatively common in the volcanic complex. The emission of three lava channels during the Holocene with their origin in areas that actually preserves mass of ice generated melting glaciers, which deposits has been identified in the NW, SE and SW sectors of the volcanic complex (Úbeda, 2010).

1.5 Glacier evolution

In the arid and semiarid regions of the tropics and subtropics more than 80% of the freshwater supply originates in mountain regions, affecting populations downstream (Messerli, 2001). Much of this water is initially stored as ice in mountain glaciers and then gradually released over time. More than 99% of all tropical glaciers are located in the Andes (Kaser, 1999). Mountain glaciers, such as those found in the tropical Andes, therefore act as a critical buffer against highly seasonal precipitation and provide water for domestic, agricultural or industrial use at times when rainfall is low or even absent. At the same time these glaciers are particularly sensitive to climate change because they are constantly close to melting conditions. They are arguably the most visible indicator of climate change, due to their fast response time, their sensitivity to climate variations and the clear visibility of their reaction (glacier growth or shrinkage) to the public. The air temperature in Central Andes has increased 0,1ºC each decade since the middle of the 20th century (Vuille et al., 2008).

There have been several studies in different Peruvian regions focused on understanding glacier chronology and glacier retreat, ultimately aiming at analyzing the processes of climate change (Giraldez, 2011). Smith et al. (2005) suggest that an absolute chronology for the last glacial cycle and ice coverage in the tropics is unavailable, largely because of the limitations of radio-carbon dating and the scarcity of datable material in glacial environments above 4000 m above the sea level (masl). Also suggest that existing glacial chronologies for the tropics are based primarily on minimum-limiting radiocarbon dates and relative dating techniques.

Giraldez (2011) pointed that the main studies in Central Andes can be classified in four glacial phases: Local Last Glacial Maximum (LLGM), Younger Dryas (YD), Little Ice Age (LIA) and modern glacier fluctuations.

Bromeley et al., (2009) reconstruct Late Pleistocene glacier fluctuations on Nevado Coropuna. Through careful reconstruction of former glacier extent and chronologic constraint of moraine records, is possible to determine both the timing and magnitude of glacier events, and therefore climate change, in glaciated and formerly glaciated regions. For observe glacier and paleo-glacier evolution is necessary to characterize the ice mass in the different phases using indicators that shows the changes in the chronology and magnitude of the glaciers. The best indicator for this purpose is the Equilibrium Line Altitude (ELA) (Úbeda et al, 2012). The ELA is an isoline that divides in the glacier the accumulation zone (where predominate the mass gain processes) and the ablation zone (where predominate the mass loss processes).

Seltzer et al. (2000, 2002) interpreted sedimentological, palaeobiotic and isotopic changes in a sediment core from Lake Junín (11º S, 76º W, ~4080 m a.s.l.) to indicate that the local LGM in the central Peruvian Andes occurred ca. 30–22.5 ka, followed by deglaciation ca. 22–21 ka and a minor readvance ca. 21–16 ka, all during wet climatic conditions, and then rapid glacial retreat as the climate became drier after 16 ka. Wet conditions returned after ca. 10 ka (Seltzer et al., 2000). According to Seltzer et al. (2002), deglaciation ca. 22–21 ka occurred as a response to increased mean annual temperatures rather than a change in the moisture regime. In some regions the glacial advances of the local LGM are relatively minor compared to older advances (Smith et al., 2005c), whereas in at least one neighbouring region ~100km away the local LGM deposits mark the outermost moraines identified (Hall et al., 2006). Differences in valley hypsometry and maximum peak altitudes seem likely to have played a role in these regional variations.

According to Smith et al. (2008) interpretation of the timing of the local LGM in the Peru and Bolivia depends to some extent on the manner in which CRN ages are calculated. Studies that have used the time-dependent Lal (1991)/Stone (2000) scaling method suggest that the local LGM in Peru (Farber et al., 2005; Smith et al. (2005b,c) and Bolivia (Smith 2005b) occurred closer to ca. 30 ka than 21 ka (that is, before the global LGM as inferred from the marine isotope record), whereas a study in Bolivia using an alternative scaling method (Lifton et al., 2005) suggests that the local LGM was closer to ca. 24 ka (Zech et al., 2007). (Smith et al., 2008) suggest the existence of widespread evidence for a stillstand or readvance after the local LGM in the tropical Andes (ca. 18– 15 ka as calculated by Smith et al., 2005c) implies a regionalscale forcing. The coincidence with wet conditions in Lake Junín (Seltzer et al., 2000, 2002) and the high stand of palaeolake Tauca on the Altiplano (Placzek et al., 2006) suggests that the cause may have been a precipitation increase. Placzek et al. (2006) speculated that the palaeolake high stand may have been linked to Pacific SST gradients, creating a La Niña effect. An early local LGM (ca. 32–28 ka) in the tropical Andes would have preceded a palaeolake high stand on the Altiplano by some 4–8 ka (Placzek et al., 2006), suggesting a different climate forcing than the ca. 18–15 ka still stand/readvance.

The studies of Mercer and Palacios (1977), Mercer (1982, 1984), Goodman et al. (2001) and Mark et al. (2002) in and around the Cordillera Vilcanota and the Quelccaya Ice Cap provide considerable radiocarbon age control for late Quaternary glaciation in this region. The outermost moraines at ~3600 m a.s.l. in the Upismayo Valley of the Cordillera Vilcanota are older than 41 520±4430 ^{14}C a BP, which is the basal age of a 10 m thick peat layer located upvalley at 4450 m a.s.l. (Goodman et al., 2001). A sample from the upper part of the same peat layer provided a maximum-limiting age of

13 880±150 ^{14}C a BP (ca. 16.7 cal. ka BP) for a group of seven nested moraines located farther upvalley (Goodman et al., 2001). Results from sediment coring provide minimum-limiting dates for deglaciation from the local LGM in the Cordillera Vilcanota. In Laguna Casercocha (4010 m a.s.l. on the northwestern side of the Cordillera in a tributary to the Upismayo Valley), organic material overlying glacial silts in a sediment core yielded a radiocarbon age of 15 640±100 ^{14}C a BP (ca. 18.5 cal. ka BP), indicating a transition from glacial to non-glacial sedimentation beginning shortly after 20 cal. ka BP (Goodman et al., 2001). In moraine-dammed Laguna Comercocha (4580 m a.s.l. approximately 6 km east of the Upismayo Valley), basal lacustrine organic material dated to 14 00±220 ^{14}C a BP (ca. 17.4 cal. ka BP; Goodman et al., 2001). Mercer and Palacios (1977) identified three moraine belts in the Huancane Valley on the west side of the Quelccaya Ice Cap and obtained a minimum-limiting age of 12 240±170 ^{14}C a BP (ca. 14.3 cal. ka BP) at 4750 m a.s.l. for the outermost belt (Huancane´ III). Additional minimum-limiting ages (e.g., Rodbell and Seltzer, 2000; Goodman et al., 2001; Mark et al., 2002) have been published for the Huancane´ moraines, but no maximum-limiting ages have been reported. Kelly and Thompson (2004) presented preliminary surface exposure ages (^{10}Be) from moraines along the margins of the Quelccaya Ice Cap. The ages were generally Lateglacial to early Holocene.

In Perú the YD appears to correspond to an interval of rapid ice retreat based on radiocarbon-dated ice margin positions in the Cordillera Blanca and in the Cordillera Vilcanota (Rodbell and Seltzer, 2000), but there is little firm evidence for glacial advances in the tropical Andes during the YD climate reversal. Also (Robell et al., 2009) suggest that in peruvian central Andes, ice was retreating during much of the remaining YD interval, but point that well-dated moraines record a significant ice re-advance at the onset of the YD.

The spatial–temporal pattern of Holocene glaciation exhibits tantalizing but incomplete evidence for an Early to Mid-Holocene ice advance in many regions, but not in the arid subtropical Andes, where moraines deposited during or slightly prior to the Little Ice Age (LIA) record the most extensive advance of the Holocene. The records obtained by Licciardi et al.(2009) in the Cordillera Vilcabamba do not exclude the possibility of multiple Holocene glacier expansions. However, the combined geomorphic and geochronologic evidence clearly indicates the dominance of two major episodes, including an early Holocene glacial interval and a somewhat less extensive glaciation during the LIA. The most precisely dated LIA maximum in the Vilcabamba (C.E. 1810 ± 20) postdates LIA maxima in the Cordillera Blanca by ~180 years, which may be explained in part by uncertainties in lichenometric and ^{10}Be exposure dating methods, but probably indicates real differences in the timing of glacial culminations (Licciardi et al., 2009).

Tropical glaciers have drastically retreated since the end of the Little Ice Age. The small glaciers — and those in Irian Jaya which extend only over a small altitude range — had the highest relative area losses, whereas the large glaciers in the Cordillera Blanca and in the Cordillera Real have had relatively small losses. This can be expected because of the year-round ablation below the equilibrium line of tropical glaciers. The respective strong vertical balance gradient leads to a substantially high sensitivity of the tongues to a rise of the ELA. Glaciers with a small altitudinal extent are obviously most effected (Kaser, 1995, 1998).

Modern ELAs in the tropical Andes have been estimated at 5000–5200 m a.s.l. (e.g. Wagnon et al., 1999). Smith et al. (2008) suggest that the steep vertical mass balance profiles of tropical glaciers result in different climate sensitivities of ELA positions along and across the Andes. Glaciers in the inner tropics have ELAs close to the 0ºC isotherm, and respond directly to temperature changes. Those in the outer tropics and

subtropics (including glaciers in the arid Western Cordillera of southern Peru and Bolivia) commonly have ELAs well above 0ºC isotherms, and thus are not as temperature-sensitive. Rather, they are more responsive to changes in precipitation and humidity that alter the sublimation/melt regime (Kaser, 2001).

Zech et al., (2008) proposed the following tentative of palaeoclimate model to explain the reviewed glacial chronologies: 1) Glaciers in the northern, tropical parts of the Central Andes were mainly temperature sensitive and advanced during temperature minima, i.e. the global LGM (ca. 20–25 ka), Heinrich event 1 (ca. 15 ka) and the Lateglacial reversals (YoungerDryas and/or Antarctic Cold Reversal, ca. 11–13 ka). 2) South and west of the Cordillera Oriental, glaciers become much more precipitation sensitive. Major advances therefore occurred during the Lateglacial, synchronous with respective lake transgression phases on the Altiplano (18–14 and 13– 11 ka). The intensification and/or southward shift of the tropical circulation even affected regions in northern Chile, 30º S, implying a southward shift of the Arid Diagonal. 3) From 30 to 40º S latitude glaciation reached a maximum extent before the global LGM at ~35–40 ka. Glaciers there were likely very sensitive to precipitation changes, and we assume an increase in extra-tropical precipitation, caused by a northward shift of the atmospheric circulation and the Arid Diagonal. 4) South of ~40º S, precipitation is much higher and glaciers become more temperature sensitive again. Accordingly, maximum glaciation occurred synchronously with the global temperature minimum of the LGM.

According to the investigation of Alcalá et al.(2011) of the Ampato Volcanic Complex, the glaciers on HualcaHualca volcano reached the minimum altitude of the whole volcanic complex during the LGM (3900 m on its northern flank) probably due to the great accumulation basin formed by the caldera opening in this direction, compared to 4300 m on its other slopes. The most important re-advance glaciers reached 4645 m on the eastern side, 4450 m on the western side and 4170 m on the northern side. Moraine ridges presumably of the LIA can be found in many of the valleys al short distance from the glacier fronts of 1955, with a mean minumum altitude of 5628 m and overall minimum altitude of 5400 m for the Ampato Volcanic Complex as a whole.
Dornbusch (1997, 2000, 2002) calculated the paleo-ELA for the LGM period in the Central Volcanic Zone, identifying moraines in the northern. His estimates range between 4600 and 5400 m for north facing slopes. On the Nevado Sara Sara he obtained a mean paleo-ELA for the LGM of ~4700 m, with a depression of 500 m compared to 1955. The corresponding values are 4970 m and 500 m for Nevado Solimana; 4750 m and 670 m for the south side of Coropuna.

Úbeda et al. (2009) obtained results on both sides of the Coropuna, similar to the results of Alcalá et al.(2011) on Hualca-Hualca, with a mean of 5070 m and a depression of around 850 m. ELA depressions for the LGM of ~1000 m have been reported in models of the general distribution of Pleistocene glaciers in the central Andes (Klein and Isacks, 1998; Hastenrath, 2009) and in specific locations such as the north-central Cordillera Oriental and the Cordillera Blanca (Rodbell, 1991, 1992)

In Queñua Ranra gorge of Nevado Coropuna, Úbeda and Palacios (2009) dated moraines similar to those of HualcaHualca in 17,0 ^{36}Cl kyr. Bromley et al. (2009) studies shows numerous LGMA moraine dating with ^{3}He, also from the Coropuna, with results ranging between 24,5 and 25,3 kyr, and between 16,7 and 21,1 kyr, respectively,depending on the cosmogenic production model used. Interestinly, in many masimum advance moraines there are boulders of both ~21,0 kyr and ~17,0 kyr.

According with Racoviteanu et al. (2007) Coropuna decreasing from 82.6 km2 in 1962 to 60.8 km^2 in 2000 and with a retreat rate of the terminus of Qori Kalis that was 10 times faster (~60myr^{-1}) between 1991 and 2005 than in the initial measuring period,

1963–1978 (Thompson et al., 2006). Since the middle of the 20th century the glacier system of Nevado Coropuna has been decreased, and is accelerating this decreasing during the last decades. According to Úbeda (2010) investigation, since 1955 to 1986 has decreased 2,1 km^2, a 3,7% in 31 years, that implies a 0,1 km^2 of loss. In the period that goes from 1986 to 2007 the glacier decreased 7,5 km^2, a 13,9% in 21 years, this suppose a deglaciation rate of 0,4 km2, 0,6% each year.
The investigation shows that between 1986 and 2007 the surface loss of the glacier system was 5,4 km^2 greater and increased by 10,2% over the three previous decades. The acceleration of the process is obvious. Actually, the summit areas of Nevado Coropuna are covered by a glacier system of almost 50 Km^2, the glaciers descend by the slopes in all directions until arrive to a elevation between 5200 and 5600 meters (Úbeda, 2010).

1.6 Aims and objectives

Is a fact that there is a lot of population living around tropical glaciers that depend of the water supply that the glaciers provide them. The live around the glaciers also implies a risk, glacial hazards and risk associated with glacier retreat, such as ice avalanches, new glacier lake formation and glacial lake outburst floods (GLOF), constitute a major cause of severe catastrophes in populated mountain areas(Huggel et al., 2004). The management of these risks is a complex task involving analysis, evaluation, and communication as well as prevention and mitigation (Greminger 2003). The tropical glaciers located on low-latitude, high-altitude mountain ranges are highly sensitive components of the environment and appear to react more immediately to fluctuations in climate than glaciers in the mid- and high-latitudes (Guilderson et al., 1994; Hostetler and Mix, 1999; Hostetler and Clark, 2000; Seltzer et al., 2002). These glaciers has a faster reaction to the climate change than mid-latitude glaciers (Solomina et al., 2007), this is why they are a key indicator for the climate change (Frey et al., 2010).

The objective of this project is to obtain information about the changes that have happened in the glaciers of the SW slope of Nevado Coropuna and analyze their evolution in two glacial phases (1955 and 2007). The methods used are geographical information technologies, particularly ESRI's ArcGIS 10 and photointerpretation. The final result has the purpose of increasing the knowledge about these glaciers.

1.7 Organization of the Thesis

This thesis is structured in four chapters, the actual is an introduction, followed by the description of the geographical information technologies applied in this project, in the second chapter. The chapter 3 presents an analysis of the results obtained, followed by a discussion of the results in the chapter 4.

CHAPTER 2

METHODOLOGY

In the present chapter, a description of the geographical information technologies applied in this project is presented: the GIS software used for the analysis was ESRI ArcGIS10 in its ArcMap environment. The first part of this chapter is followed by a presentation of the materials needed for the analysis and the necessary steps for complete all the methodological phases: georeferentiation, moraine mapping, glacier and paleo-glacier delimitation, surface calculation and ELA and paleo-ELA calculation.

(1): Georeferentiation, one of the ArcGIS software characteristics is the stacking of georeferenced data in layers in order to establish comparisons, this first step is very important because is the basis of all the subsequent work.

(2): Moraine mapping, in this part of the work the moraines were digitalized following the traces that the paleo-glaciers left behind, was the step from which to delimit paleo-glaciers in the LLGM glacial phase.

(3): Glacier and paleo-glacier delimitation, for establish the glacier limits was necessary the interpretation of satellite and aerial photographs, in the case of paleo-glaciers the reconstruction was made starting from moraine mapping.

(4): Surface calculation and ELA and paleo-ELA calculation: for check the evolution of the glaciers was necessary to calculate this imaginary line in order to establish the limits of the ablation zone and accumulation zone of the glaciers, the application of some equations (collected on a spreadsheet) was required for this purpose.

2.1 Materials

A list of materials used for the analysis is the following:

Source	Data
IGN (Instituto Geográfico Nacional de Perú)	Aerial photographs 1955
GFAM-GEM	ASTER image 2007
Google	Google Earth mosaic
GFAM-GEM	Contour lines
GFAM-GEM	AABR Spreadsheet (Osmaston 2005)
GFAM-GEM	Moraine situation

The aerial photographs obtained from the 1955 flight were obtained from IGN (Instituto Geográfico Nacional de Perú) and were used for the 1955 glacier delimitation.

The ASTER image and was used for the 2007 glacier delimitation combined with Google Earth mosaic. High resolution mosaic of the West Slope of Nevado Coropuna was elaborated from Google Earth images and was used also for calculate the glacier delimitations.

The contour lines of the Nevado Coropuna were obtained from GFAM-GEM. An excel spread sheet used for the AABR calculation was made by Osmaston (2005) and provided by GFAM-GEM

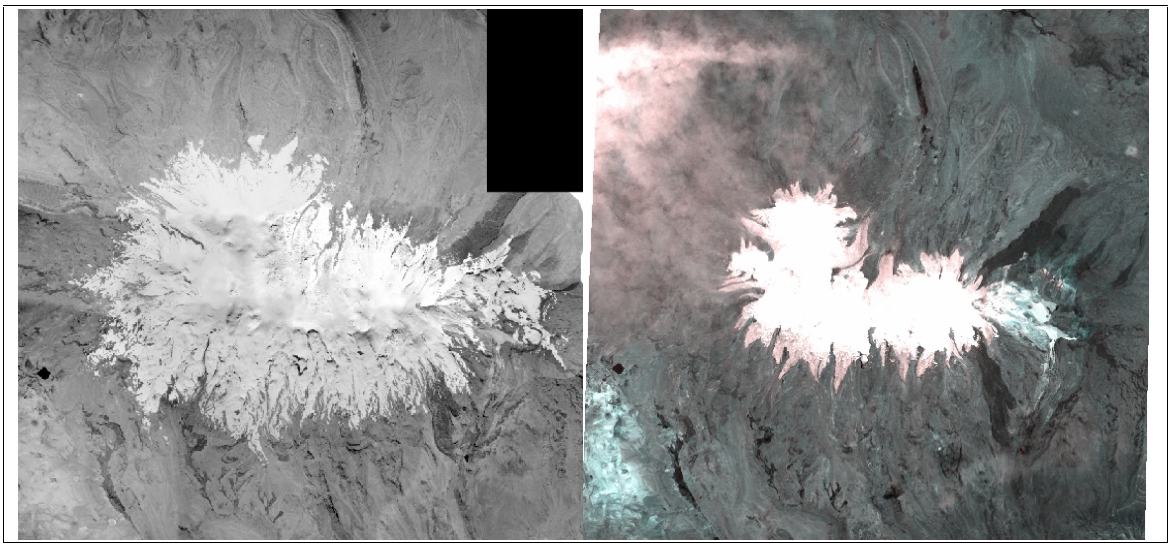

Figure 2. 1. From left to right, image from 1955 flight and ASTER image 2007.

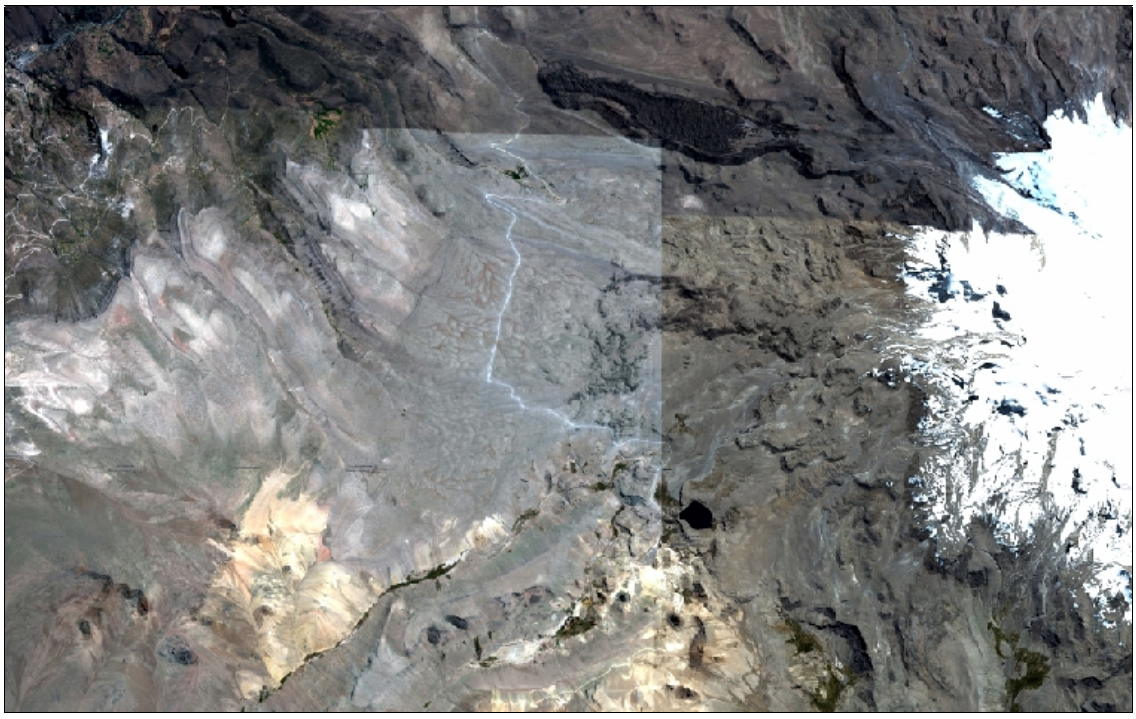

Figure 2. 2. Google Earth mosaic provided by GFAM-GEM

2.2 Georeferencing

The images used in this analysis had been georeferenciated previously by GFAM-GEM. The aerial photographs from 1955, previously to the georeferencing process were scanned in high resolution and converted to raster files. The "Georeferencing" toolbar options of ArcMap were used for this geocoding process. Coordinates had been assigned to points of the image of known locations that were distinguished on a georeferenced image used as a control layer. This control points helps to "fit" the image in the coordinates in the "Rectify" step of the georeferencing. At the end of this process a georeferenced image were obtained.

The accuracy of the transformation is evaluated with the Root Mean Square error (RMS), which measures the accuracy of control points and can be used to find and delete inaccurate entries. Once at least four control points have been added, RMS error will be calculated for each entry. Basically, residual error is the measure of fit between the true and transformed locations of the control points. Depending on the number of control points, is possible to perform either a 1^{st}, 2^{nd}, or 3^{rd} order transformation. These transformations compare the coordinates of the source image with the control points creating two least-square fit equations to translate the image coordinates into map coordinates. A 1^{st} order transformation shifts the image up, down, right, or left, stretches the image larger or smaller, or rotates the entire image. The 2^{nd} and 3^{rd} order transformations fit higher-order polynomial equations to the data, allowing points to be shifted in a non-uniform manner.

2.3 Moraine mapping

Once the reference images were properly geocoded, the first step in the process of reconstructing Ice Age glaciers is to establish the geometry of the paleo-glaciers from which other characteristics and mechanisms can be deduced (Haeberli, 2010). The moraine mapping used in this analysis has been done previously by GFAM-GEM. The mapping was done with photointerpretation techniques using a stereoscope with aerial photographs, also Google Earth helps in the interpretation process. Once the moraines were identified, the next step was the digitalization process with the ArcGIS software, the digitalization of the moraines were done over a Google Earth mosaic using the "Editor" toolbar and its options.

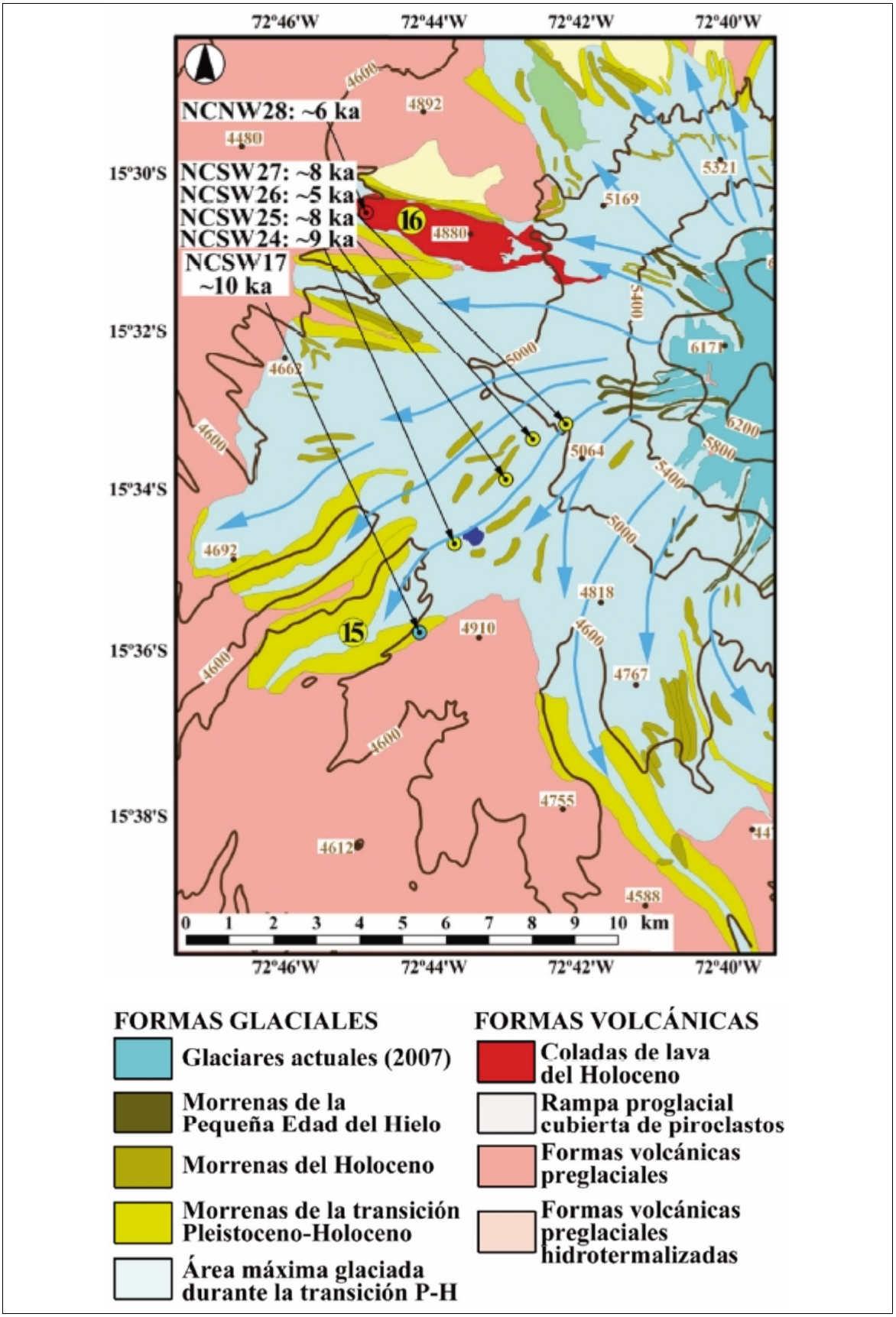

Figure 2. 3. Moraine mapping over W slope of Nevado Coropuna, with volcanic forms and information about actual and paleo glaciers (GFAM-GEM).

From the mapped moraines the glacier delimitation is the next step of the analysis.

2.4 Glacier delimitation and surface calculation

The glacier delimitation process is based in the interpretation of the Google Earth mosaic and aerial photographs (using also in this case a stereoscope), in order to establish the limits and calculate the surface of the glaciers. In the case of paleo-glaciers, moraine mapping is used for their delimitation.

According to Ben et al. (2005), reconstructing the former extent of glaciers requires detailed geomorphic mapping and the analysis of landforms and sediments. The most accurate methods also require that there is sufficient geomorphic evidence, usually lateral-terminal moraines and trimlines, to allow the shape of the former glacier to be reconstructed. However, glacial moraine evidence is by nature discontinuous; and relatively younger and larger advances of a glacier will destroy moraines deposited in older, less-extensive advances, leaving an incomplete geomorphic record. Lake sediments down-valley from the moraines may provide an important source of data to help reconstruct glacier front oscillations, but it cannot automatically be assumed that clastic sediment peaks in lacustrine records correspond to glacial maxima, rather than paraglacial sediment reworking during deglaciation (Ballantyne, 2002). If is possible, is important to use images of the dry season, because there was no snow over the ice and the glaciers are clearly visible. If the snow covers the glacial ice is difficult to recognize the limits of the glaciers. For the 1955 glacier delimitation, a careful interpretation has been done, because the images from the aerial flight were not taken in the dry season and the glacial ice was partially covered by the snow. In the 2007 process, the ASTER image was taken in October and there is no snow over the ice.

Would be suitable a paleo-glacier reconstruction based on field observations, aerial photographs, satellite imagery and high-resolution digital topographic data, however it was not possible to make field observations for this reconstruction, this phase of the analysis was done with Google Earth mosaic observation combined with aerial photographs and using also the topographic contour lines.

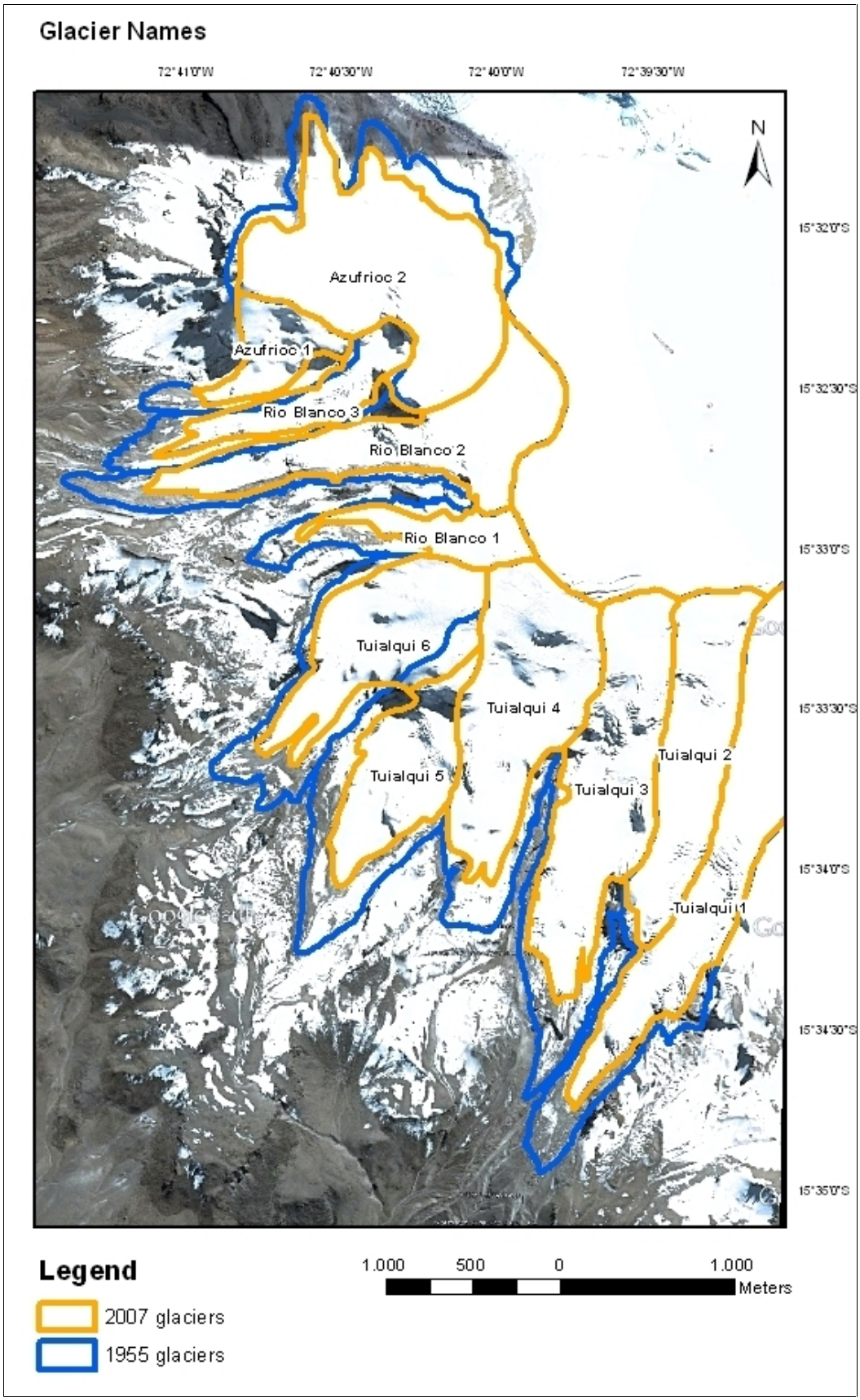

Figure 2. 4. Names given to glaciers over Google Earth mosaic

2.5 ELAs AABR

The ELA (Equilibrium Line Altitude) is an imaginary line that separates the ablation zone and the accumulation zone. At this altitude, the amount of new snow gained by accumulation is equal to the amount of ice lost through ablation. According to Paterson (1994), traditional definitions of the ELA refer to the altitude where bn = 0, where bn is the net balance at the end of the (summer) ablation season. This definition was developed for mid- and high-latitude glaciers, but is less obviously applicable to tropical glaciers where there is year-round ablation. Where there is a distinct dry season, the end of the dry season provides a convenient end point for the balance year. The altitude of the equilibrium line is rarely constant across a glacier, but varies with patterns of snow accumulation, shading, and other factors (Benn et al., 2005).

There are several methods for reconstructing former glacier ELAs, the methods in common use are: (1) Accumulation Area Ratios (AAR); (2) Area Altitude Balance Ratios (AABR); (3) Maximum Elevation of Lateral Moraines (MELM); (4) Terminus to Head Altitude Ratios (THAR); and (5) gross morphological indices such as glaciation threshold and cirque floor altitudes. The first two methods are based on assumed forms of the glacier mass–balance gradient, and are therefore broadly compatible with the concept of the steady-state ELA as defined above. MELM makes use of the fact that formation of moraines only occurs below the contemporary ELA, and therefore gives a minimum altitude. THAR invokes general relationships between glaciers and basin relief, but without reference to assumed mass–balance curves (Benn et al., 2005). Úbeda (2010) distinguishes morphometric methods for the paleo-glaciers reconstruction and statistical methods for current and former glaciers.

The Area Altitude (AA) and Area Altitude Balance Ratio (AABR) methods take account of the hypsometry (the detailed distribution of surface area with respect to altitude) of a glacier, unlike other methods in general use. All are based on the principle that parts of a glacier which are far above or below the ELA have greater spot net balances (plus or minus) and so have more influence on the total mass balance of a glacier, and hence on the ELA, than those which are close. Thus they require knowledge of the position of the margin of a glacier and contour data for its surface, so that the area and mean altitude of successive contour belts of its surface can be determined (Osmaston, 2005). Úbeda (2010) chose the AA and AABR methods for calculate the ELAs and paleo-ELAs in his investigation of the glaciers and paleo-glaciers of the NE and NW slope of Nevado Coropuna. Osmaston (2005) suggest that within statistical methods the AABR is considered to be rigorous and reliable. For these reasons, the AABR method was used in this project for calculate the ELAs and paleo-ELAs of glaciers of the SW slope of Nevado Coropuna. According to the explanation of Osmaston (2005) AABR method is based on the principle of weighting the mass balance in areas far above or below the ELA by more than in those close to it. However this is then refined by providing for different linear slopes of the mass balance/altitude curve above and below the ELA. Many glaciers conform roughly to this specification, and it serves as a useful first approximation for former glaciers for which there is no a priori knowledge about their mass balance.

2.5.1 ELAs AABR of 1955 and 2007 glaciers.

For the application of the ELAs AABR method the glacier delimitation (previously calculated) and contour data for its surface were required. The contour data were contour lines with 50 m resolution transformed into contour belts. For the generation of a contour belt the area between two contour lines was calculated. ArcGIS10 in its ArcMap environment was used for the creation of the contour belts, which had to be contained in a polygon shapefile in order to calculate each surface area. For this process was necessary the use of three ArcGIS tools: (1) Intersect; (2) Feature to Polygon, (3) Clip.

(1): The contour lines covers more surface than that needed, is for this reason that the Intersect tool (ArcToolbox → Analysis Tools → Overlay → Intersect) was used. This tool computes a geometric intersection of the input features. Features of portions of features which overlap in all layers and feature classes were written to the output feature class. The contour lines and the area of study (polygon representing the glacier delimitation) were introduced as an input features and the output was a shapefile with the contour lines of the area of study.

(2): Once a shape with the contour lines was created, next step was to obtain the contour belts of the study area, for this purpose the Feature to Polygon tool was used (ArcToolbox → Data Management Tools → Features → Feature to Polygon). This tool creates a feature class containing polygons generated from areas enclosed by input line or polygon features. The result of the previous step (contour lines of the study area) was used as the input and the output was a shapefile with the contour belts of the same area.

(3): The last step was the obtaining of the contour belts individually for each single glacier. The Clip tool was used for this purpose (ArcToolbox → Analysis Tools → Extract → Clip), this tool extracts input features that overlay the clip features, cut out a piece of one feature class using one feature in another feature class. The contour belts of the study area calculated in the step before and the selected glacier polygon (as a clip feature) were used as the inputs for the Clip operation, the output result was a shapefile with the contour belts of the selected glacier. This process has to be repeated for each glacier. The field “Area” of the Attribute table of the shapefile had to be recalculated.

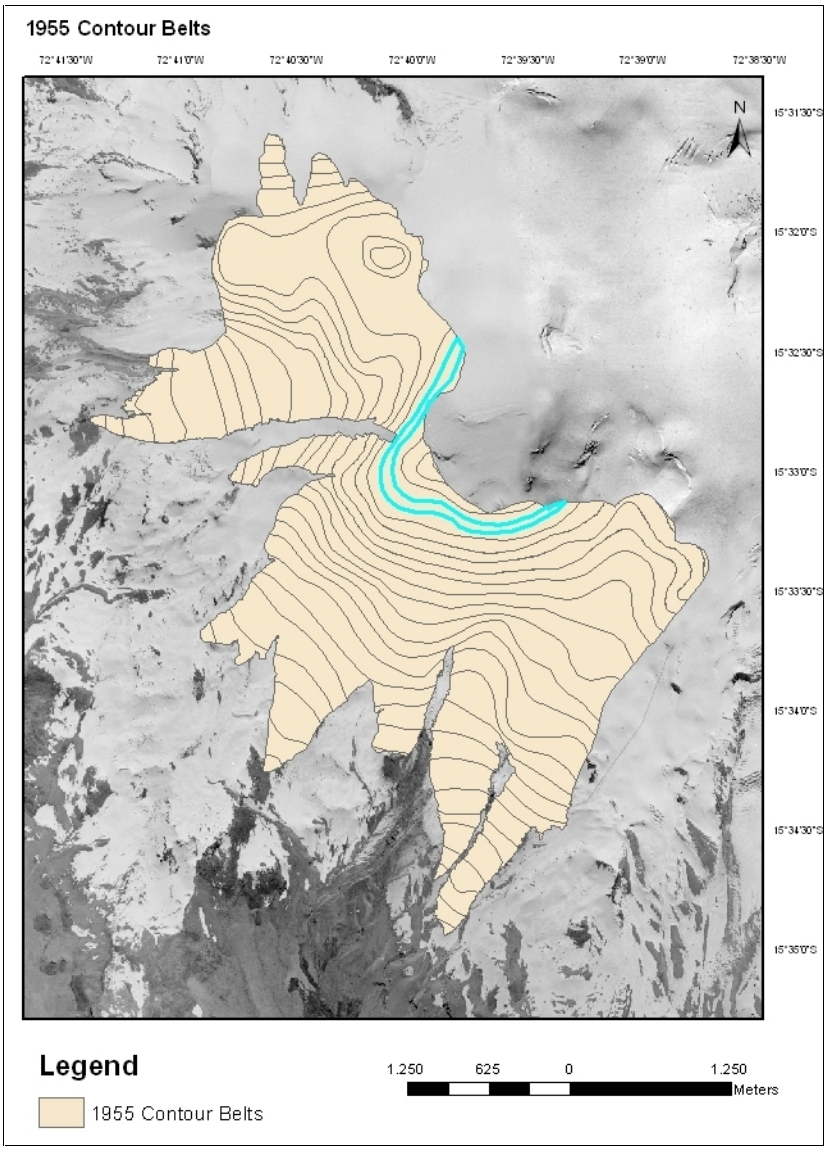

Figure 2. 5. 1955 Contour belt sections

1955 Contour Belts

Shape	Interval	MeanZ	Area
Polygon	6050-6100	6075	221197,718289
Polygon	6050-6100	6075	544868,928041
Polygon	6100-6150	6125	233174,809621
Polygon	6100-6150	6125	57020,22285
Polygon	6150-6200	6175	205720,03497
Polygon	6150-6200	6175	35702,58745
Polygon	6200-6250	6225	130643,193422
Polygon	6200-6250	6225	19405,276994
Polygon	6250-6300	6275	15156,436437

Figure 2. 6. Attribute table with the selected contour belt (6150-6200 m)

At this point, the calculations were completed with a programmed spreadsheet. The attribute tables of the shapefiles of the glaciers' contour belts were exported as a .dbf archive in order to open it with the spreadsheet for the AABR method. According to

Osmaston (2005), Sissons (1974, 1980) rediscovered the AA method, he greatly simplified the calculation by the insight that the ELA it yielded is the median value of the product of the area and mean altitude of successive contour belts of the glacier surface (not the median altitude which is the centre value of the altitude range).

Osmaston (2005) developed a method that refined Sissons (1974, 1980) idea by providing for different linear slopes of the mass balance/altitude curve above and below the ELA. Many glaciers conform roughly to this specification, and it serves as a useful first approximation for former glaciers for which there is no a priori knowledge about their mass balance. Benn and Gemmell (1997) provided a spread sheet for calculating ELAs by this method. The programme was in two parts. The first was a calculation of the ELA by the short AA method; this gave a good preliminary estimate of the ELA and was so simple that was unlikely that any error would occur in it. Thus it could be used as a general check on results, and in particular it should be equal to the AABR when BR = 1. An automatic internal check was provided using this relationship. The second part estimated the ELA by the full iteration procedure using a series of trial contour altitudes for the ELA and for each calculated the net balance of the whole glacier. These results were then reviewed and the pair at which the balance changes sign was selected. The exact ELA between these values was then estimated by the proportions of the two net balances.

The following procedure for AABR presented by Osmaston (2005) were applied in this project:

1. Check correct operation of spread sheet with trial data.

2. Check that contour table will cover glaciers to be examined and that VI is correct.

3. Enter contour belt area table for glacier 1, the fields “Z interval”, “Mean Z” and “Area” in the columns D, E and F respectively.

4. Enter altitude of first trial reference contour.

5. Enter BR = 1 and check correct operation of programme.

6. Record ELA.

7. Enter in succession a series of BR values (e.g. 1, 1.5, 2.0, 2.5, 3.0) and record the ELA for each. Ratios can be selected by a priori knowledge of what is likely; most glaciers are likely to have BRs of 1.5–3.5, though on a debris-covered one it may be less than 1.

8. Repeat for the other glaciers.

9. Enter results in a spread sheet for displaying them and calculating the mean and standard deviation of the estimated ELAs for each BR value.

10. Select the BR with the lowest standard deviation, which indicates the ELA with the best statistical probability of being correct.

11. Plot the ELAs on a map to see if they show any pattern of grouping, clines or sloping surfaces and re-analyse the data accordingly.

Table 2.1. AABR spreadsheet for glacier Rio Blanco 2 in 2007.

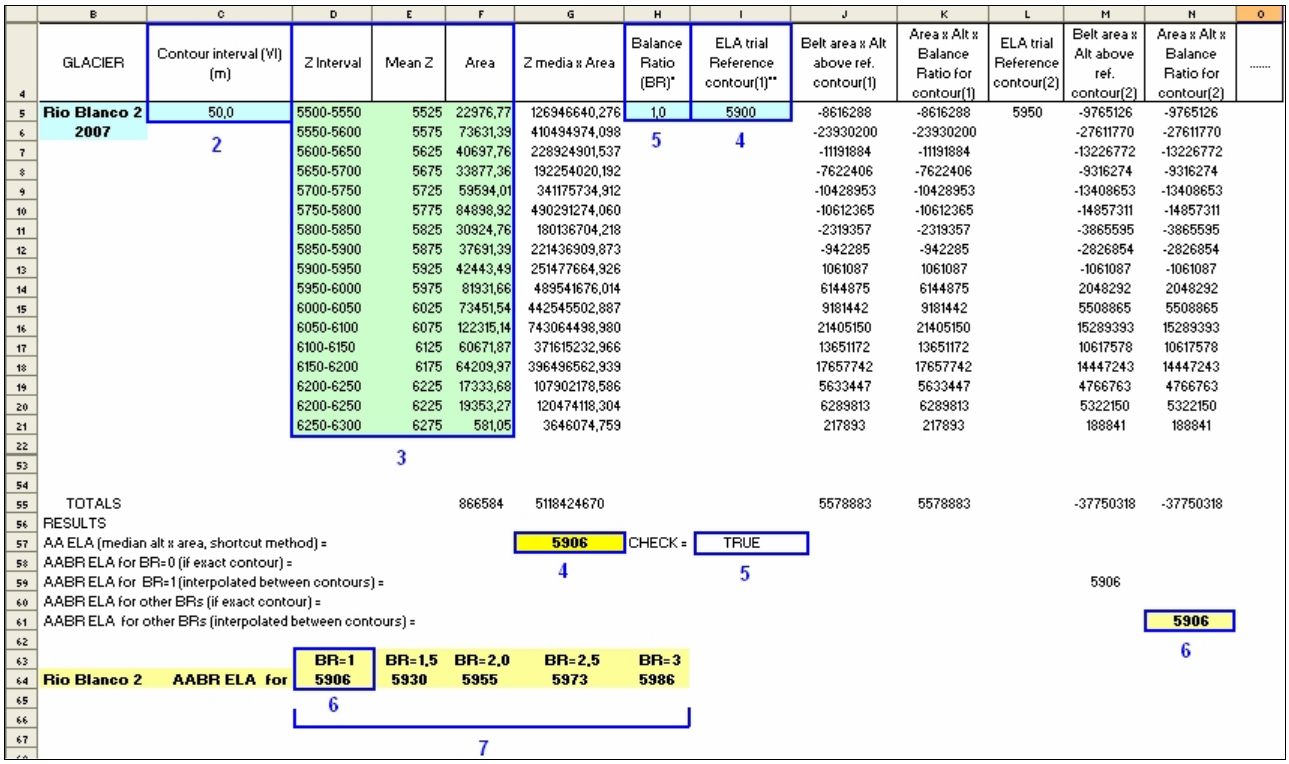

GLACIER	Contour interval (VI) (m)	Z Interval	Mean Z	Area	Z media x Area	Balance Ratio (BR)*	ELA trial Reference contour(1)**	Belt area x Alt above ref. contour(1)	Area x Alt x Balance Ratio for contour(1)	ELA trial Reference contour(2)	Belt area x Alt above ref. contour(2)	Area x Alt x Balance Ratio for contour(2)	.....
Rio Blanco 2	50,0	5500-5550	5525	22976,77	126946640,276	1,0	5900	-8616288	-8616288	5950	-9765126	-9765126	
2007	2	5550-5600	5575	73631,39	410494974,098	5	4	-23930200	-23930200		-27611770	-27611770	
		5600-5650	5625	40697,76	228924901,537			-11191884	-11191884		-13226772	-13226772	
		5650-5700	5675	33877,36	192254020,192			-7622406	-7622406		-9316274	-9316274	
		5700-5750	5725	59594,01	341175734,912			-10428953	-10428953		-13408653	-13408653	
		5750-5800	5775	84898,92	490291274,060			-10612365	-10612365		-14857311	-14857311	
		5800-5850	5825	30924,76	180136704,218			-2319357	-2319357		-3865595	-3865595	
		5850-5900	5875	37691,39	221436909,873			-942285	-942285		-2826854	-2826854	
		5900-5950	5925	42443,49	251477664,926			1061087	1061087		-1061087	-1061087	
		5950-6000	5975	81931,66	489541676,014			6144875	6144875		2048292	2048292	
		6000-6050	6025	73451,54	442545502,887			9181442	9181442		5508865	5508865	
		6050-6100	6075	122315,14	743064498,980			21405150	21405150		15289393	15289393	
		6100-6150	6125	60671,87	371615232,966			13651172	13651172		10617578	10617578	
		6150-6200	6175	64209,97	396496562,939			17657742	17657742		14447243	14447243	
		6200-6250	6225	17333,68	107902178,586			5633447	5633447		4766763	4766763	
		6200-6250	6225	19353,27	120474118,304			6289813	6289813		5322150	5322150	
		6250-6300	6275	581,05	3646074,759			217893	217893		188841	188841	
			3										
TOTALS				866584	5118424670			5578883	5578883		-37750318	-37750318	
RESULTS													
AA ELA (median alt x area, shortcut method) =					**5906**	CHECK =	TRUE						
AABR ELA for BR=0 (if exact contour) =					4		5						
AABR ELA for BR=1 (interpolated between contours) =											5906		
AABR ELA for other BRs (if exact contour) =													
AABR ELA for other BRs (interpolated between contours) =												**5906**	
												6	
		BR=1	BR=1,5	BR=2,0	BR=2,5	BR=3							
Rio Blanco 2	**AABR ELA for**	**5906**	**5930**	**5955**	**5973**	**5986**							
		6											
		7											

In the step 4, column I contains the altitude of the first reference contour line immediately below the first ELA value obtained with an AA ELA shortcut method presented by Sisson (1974, 1980):

$$ELA = Z * A / A$$

The column L represents the contour line above the reference contour line in column I, the table repeats columns D, E and F for successive values of trial ELA until 10 trials.

Once obtained the results, these were introduced in other spreadsheed in order to obtain the mean and standard deviation of the estimated ELAs for each BR value. After obtaining these parameters the BR with lowest standard deviation was selected, which indicated the ELA with the best statistical probability of being correct.

Table 2.2. Spreadsheet for the calculation of the standard deviation of ELAs.

QUEBRADA TUIALQUI	BR=1	BR=1,5	BR=2,0	BR=2,5	BR=3
Tuialqui 1	5746	5706	5723	5746	5764
Tuialqui 2	5819	5807	5825	5838	5847
Tuialqui 3	5700	5739	5763	5779	5791
Tuialqui 4	5889	5852	5872	5890	5903
Tuialqui 5	5579	5560	5552	5561	5568
9 Tuialqui 6	5814	5819	5841	5857	5868
MEAN	5758	5747	5763	5779	5790
STANDARD DEVIATION	109	106	117	119	120

QUEBRADA RIO BLANCO	BR=1	BR=1,5	BR=2,0	BR=2,5	BR=3
Rio Blanco 1	6102	6128	6150	6165	6177
Rio Blanco 2	5906	5930	5955	5973	5986
9 Rio Blanco 3	5767	5753	5768	5777	5785
MEAN	5925	5937	5958	5972	5983
STANDARD DEVIATION	168	188	191	194	196

QUEBRADA AZUFRIOC	BR=1	BR=1,5	BR=2,0	BR=2,5	BR=3
Azufrioc 1	5825	5804	5810	5820	5828
9 Azufrioc 2	6026	6015	6007	6002	6002
MEAN	5926	5910	5909	5911	5915
STANDARD DEVIATION	142	149	139	129	123

GENERAL SW SLOPE	BR=1	BR=1,5	BR=2,0	BR=2,5	BR=3
MEAN	5834	5828	5842	5855	5865
STANDARD DEVIATION	146	154	157	156	156
9	10				

2.5.2 Paleo-ELAs AABR of paleo-glaciers.

For calculate the paleo-ELAs AABR for the paleo-glaciers the same procedure was applied, but for this case a step was added at the beginning of the process. The contour lines were modified for the paleo-glaciers representation due to the non existence of the paleo-glaciers when the contour lines were created. Giraldez (2011) pointed what in current topography appears as glacier eroded valleys, it is assumed that in former times were filled with glaciers. For this reason, the contour lines should be adjusted to a hypothetical reconstruction of the ice surface and volume. Each contour line had been modified.

For the reconstruction of the paleo-topography the ArcGIS10 in its ArcMap environment was used. The use of the following tools was necessary: (1) Clip; (2) Editor, (3) Erase, (4) Merge.

(1): The first was the obtaining of the paleo-glacier limits with their contour lines. The original contour lines were used as the input for the Clip operation, the output result was a shapefile with the contour lines in the paleo-glacier limits.

(2): Due to the changes that the topography inside the glaciers was experimented, a modification of the original contour lines was realized, for this purpose the options of the "Editor" toolbar were used in order to obtain reconstructed contour lines inside the paleo-glacier limits.

(3): Next step was to obtain the contour lines of the study area without the inside contour lines of the paleo-glacier, the tool Erase was used for this operation (ArcToolbox → Analysis Tools → Overlay → Erase), this operation created a feature class by overlaying the input features (original contour lines of the study area) with the polygons of the Erase features (inside contour lines of the paleo-glacier). Only those portions of the input features falling outside the erase features outside boundaries were copied to the output feature class.

(4): The tool Merge (ArcToolbox → Data Management Tools → General → Merge) was used to combine the erased contour lines of the study area with the previously created hypothetical contour lines of the former glaciers. The output obtained was a shapefile with the hypothetical topography of the study area in the paleo-glacial phase.

After the reconstruction of the paleo-topography, the contour belts had to be created. For this purpose the tools (1) Feature to Polygon and (2) Clip were used.

(1): The reconstructed paleo-topography and the study area were introduced as inputs of the operation and the contour belts of the study area were obtained.

(2): Using the Clip tool with the output of the preceding operation and the selected paleo-glacier the contour belts of the paleo-glacier were obtained.

These steps had to be repeated for each paleo-glacier and the area was calculated.

At this point, like in the section 2.5.1, ELA AABR calculations were completed in the spread sheet. The mean and standard deviation were calculated with the obtaining of the weighted ELAs by different Balance Ratio.

2.6 Spatial model of ELAs and accumulation and ablation zones

Several possible values were offer the calculation of ELAs AABR, one for each BR value. According to Osmaston (2005) method, the selection of the BR with the lowest standard deviation, which indicates the ELA with the best statistical probability of being correct. Osmaston pointed that a homogeneous group of glaciers should react similarly to the climate they experience. Therefore their ELAs should be closely similar, differentiated only by such local individual factors as shading by valley-side precipices. Osmaston (2005) commented that in statistical terms the standard deviation of these individual ELAs from the group mean value will be less than that of other possible sets of ELA estimates from their means. Therefore for each input value of the ratio or index set we should calculate the standard deviation of its predictions (or the standard error of the mean), and select the value which has the smallest standard deviation.

2.6.1 ELAs spatial model

For the calculating of the ELA the software ArcGIS10 in its ArcMap environment was used. The use of the following tools was necessary: (1) Dissolve; (2) Create TIN, (3) Surface Contour, (4) Intersect. These operations were done for each glacial phase treated in the present project (LLGM, 1955, 2007).

(1): The first step was the creation of a shapefile containing the outermost limits of glaciers. The tool Dissolve (ArcToolbox → Data Management Tools → Generalization → Dissolve) was used with the glacier limits input.

(2): The contour lines used have an interval of 50 m and for the ELAs altitudes a lower interval was needed (1 m), for this reason the Create TIN tool (ArcToolbox → 3D Analyst Tools → TIN Management → Create TIN) was used with the contour lines of the study area as an input of the operation. TIN (Triangular Irregular Netwoks) are a digital means to represent surface morphology and allow to model heterogeneous surfaces efficiently with higher resolution in areas where a surface is highly variable or where more detail is desired, in this case the glacier surface. A model with 50 m resolution contour line was created.

(3): The Surface Contour operation creates a feature class containing a ser of contours generated from a TIN surface, the output feature class is 2D and contains an attribute with contour values. From the 50 m resolution layer obtained previously, the Surface Contour tool (ArcToolbox → 3D Analyst Tools → Terrain and TIN surface → Surface Contour) provided a contour line layer with 1 m resolution.

(4): The Intersect tool (ArcToolbox → Analysis Tools → Overlay → Intersect) was used for mapping the ELAs in the glacial phases. For obtain the ELA spatial model the outermost glacier limits and the 1 m contour line (representing the ELA) were used as an input of the operation. For the selection the single 1 m contour line the Select by attributes tool from the tool bar was used (Selection → Select by attributes) to select the desired contour line. This process had to be repeated for each glacial phase.

2.6.2 Accumulation and ablation zones spatial model

As described previously in this project, the ELA is an imaginary line that separates the ablation zone and the accumulation zone. At this altitude, the amount of new snow gained by accumulation is equal to the amount of ice lost through ablation. The accumulation and ablation zones were deduced dividing in two different polygons the polygon that formed the outermost glacier limits by the ELA line.

For this operation these tools were used: (1) Polygon to Line; (2) Editor; (3) Merge; (4) Feature to Polygon.

(1): The outermost glacier limits polygon was converted into poly-line feature with the Polygon to Line tool (ArcToolbox → Data Management Tools → Features → Polygon to Line).

(2): The Editor toolbar and its Split tool (Editor → Split) were used for cut the glacier poly-lines over the intersection with the ELA.

(3): The tool Merge was used to combine the glacier poly-lines over the intersection with ELA with the ELA poly-line. The output obtained was a shapefile with a single poly-line layer.

(4): Once the shapefile with a single poly-line was created, next step was to obtain the accumulation and ablation spatial model, for this purpose the Feature to Polygon tool was used. From the single poly-line layer with accumulation selected lines a polygon was created. The same process was done for the creation of the ablation spatial model. This process had to be repeated for each glacial phase.

2.6.3 Surface calculation

A new field was added in the attribute tables of the single polygons for the calculation of the accumulation and ablation zones surfaces, in this field the surfaces were calculated (in km^2) with the “Calculate Geometry” tool in the corresponding column of the attribute table.

CHAPTER 3

RESULTS

Glaciers are good indicators of the climate change, they are also an important supply of resources for the population who is living there. The purpose of this project was to reconstruct glaciers on the SW slope of Nevado Coropuna in several glacial phases through photointerpretation and moraine mapping (for paleo-glacier reconstruction), and calculate the glacier surfaces and their ELAs in order to analyze the glacier evolution and achieve valuable information of the changes that have happened. The following results explain the methodology used for these purposes, first the moraine mapping, followed by the glacier delimitation and their surface calculation and finally the calculation of ELAs and the accumulation and ablation zones of the glaciers.

3.1. Moraine mapping

The moraines are a geomorphological evidence of the movements of the glaciers in the past, from the moraines distribution is possible the paleo-glacier reconstruction.

In figure 3.1 the moraine cartography of the zone of study is presented over a LANDSAT image. The Local Last Glacial Maximum (LLGM) moraines were mapped between 4450 and 4700 m. The mapping range of the Holocene moraines was between 4750 and 5000 m, and the Little Ice Age moraines were mapped between 5200 and 6100 m.

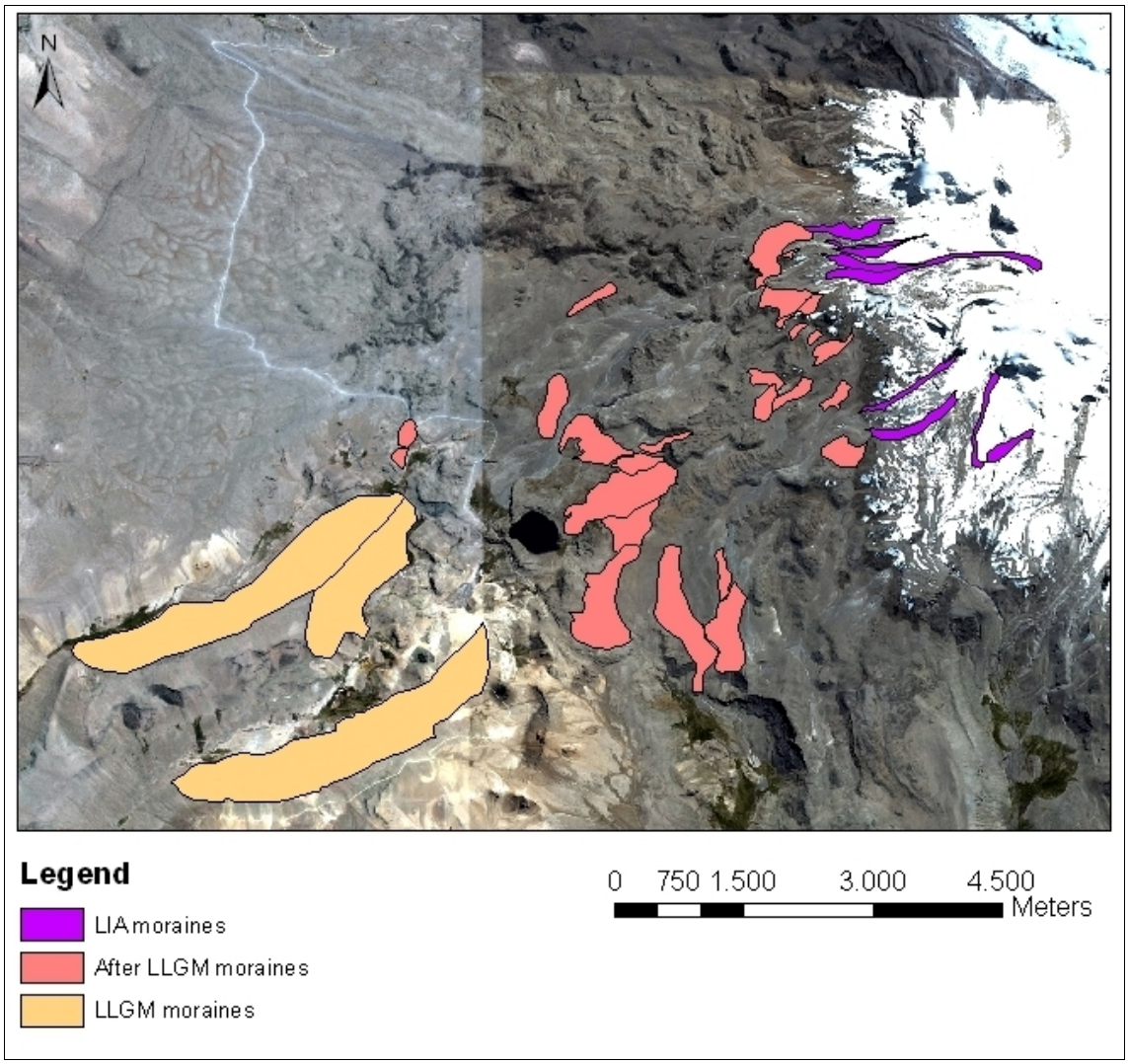

Figure 3. 1. Moraine mapping of the zone of the paleo-glaciers calculated in this work.

3.2 Glacier delimitation and surface calculation

Two delimitation phases were established for the glaciers of the SW slope of Nevado Coropuna: 1955 and 2007. Figure 3.2 shows the 1955 and 2007 glacier limits over Google Earth image mosaic. Reference materials to delimit glaciers in 1955 were aereal photographs and Google Earth mosaic for 2007 delimitation.

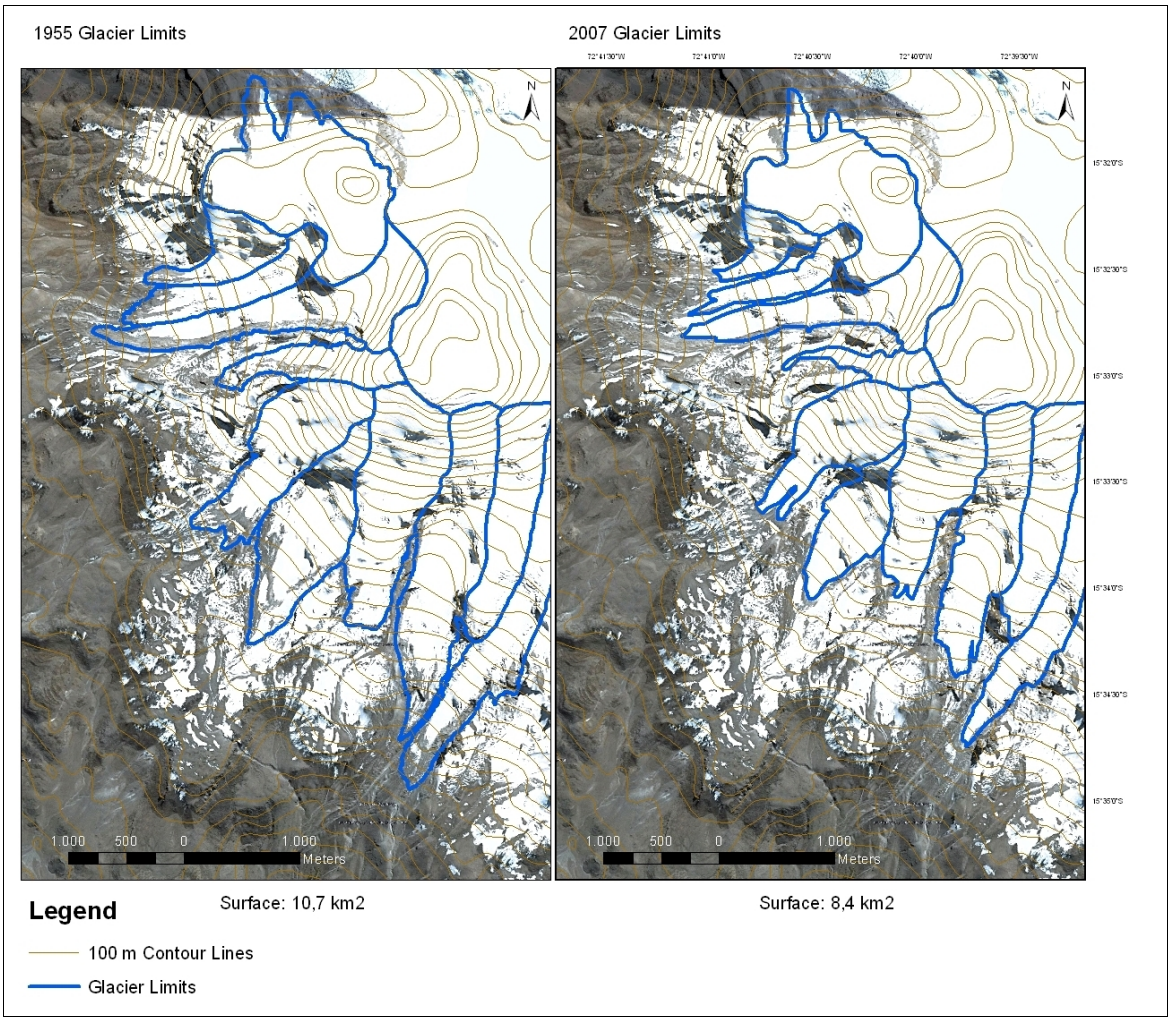

Figure 3. 2. 1955 and 2007 glacier limits over Google Earth image mosaic

In 1955 the upper glacier limits were above 6350 m for Rio Blanco 1 and lower glacier limit was 5050 m for Tuialqui 1. In 2007, for the same glaciers, the limits were above 6350 m and lower glacier limit 5150 m.

The figure 3.3 shows that the total glaciated surface in 1955 was 10,7 km^2, the surface decreased until 8,4 km^2 in 2007, this means a 21,5% retreat of the total glaciated surface in 1955.

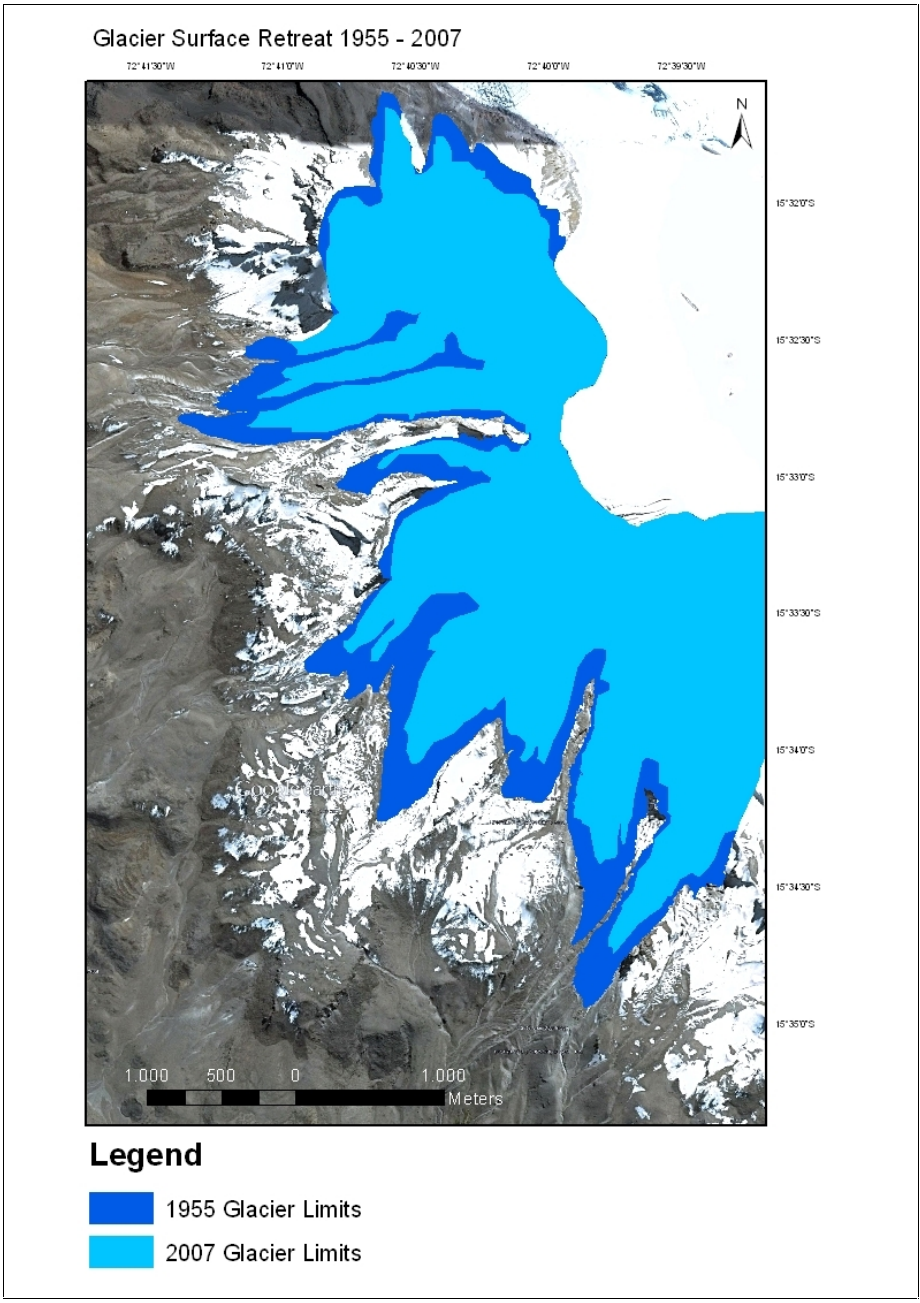

Figure 3. 3. Comparison of the glaciated area in 1955 and 2007

Individually the glaciated area retreat are showed in the table 3.1, Tuialqui 5 is the one with the maximum glaciated are retreat with 46,39% and Tuialqui 2 only loss 2,56% of their glaciated area.

Table 3.1. Glaciated area retreated in each glacier in 2007 regarding 1955.

	1955	2007	Glacier retreat (Km^2)	%	% of 1955
Tuialqui 1	1,63	1,39	0,24	14,72	85,28
Tuialqui 2	0,78	0,76	0,02	2,56	97,44
Tuialqui 3	1,3	1,02	0,28	21,54	78,46
Tuialqui 4	1,17	0,98	0,19	16,24	83,76
Tuialqui 5	0,97	0,52	0,45	46,39	53,61
Tuialqui 6	0,92	0,73	0,19	20,65	79,35
Rio Blanco 1	0,42	0,24	0,18	42,86	57,14
Rio Blanco 2	1,07	0,87	0,2	18,69	81,31
Rio Blanco 3	0,49	0,33	0,16	32,65	67,35
Azufrioc 1	0,39	0,26	0,13	33,33	66,67
Azufrioc 2	1,56	1,3	0,26	16,67	83,33
TOTAL:	10,7	8,4	2,3	21,50	78,50

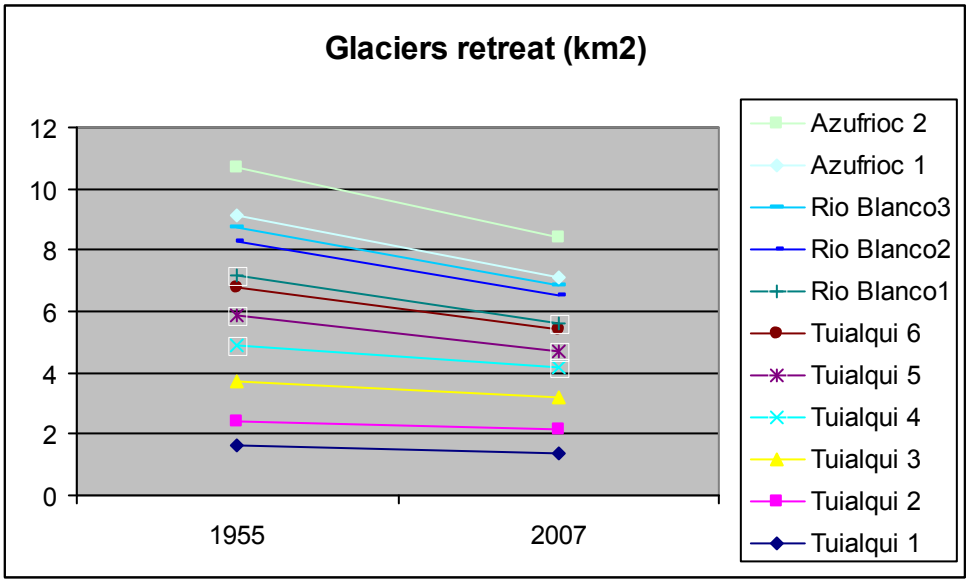

Figure 3. 4. Comparison of the evolution of each glacier

The glaciated area has been retreated in all the glaciers, one more than others, in 2007 was a total glaciated area of 78,5% (8,4 km^2) of the total glaciated area in 1955 (10,7 km^2).

These calculations of the glacier evolution were possible mapping de limits of the glaciers and their surfaces from aerial photographs and satellite images.

3.3 ELAs ABBR

For the estimation of the climate change Benn et al. (2005) pointed that the difference in altitude between modern and former ELAs has been widely used.

The glacier delimitation and contour data for its surface were required for the application of the AABR method. Osmaston's spreadsheed was used for the calculation of ELAs and paleo-ELAs, in the case of paleo-ELAs the topography was reconstructed previously. Figure 3.5 shows the reconstructions of the topography for the paleo-ELA calculation.

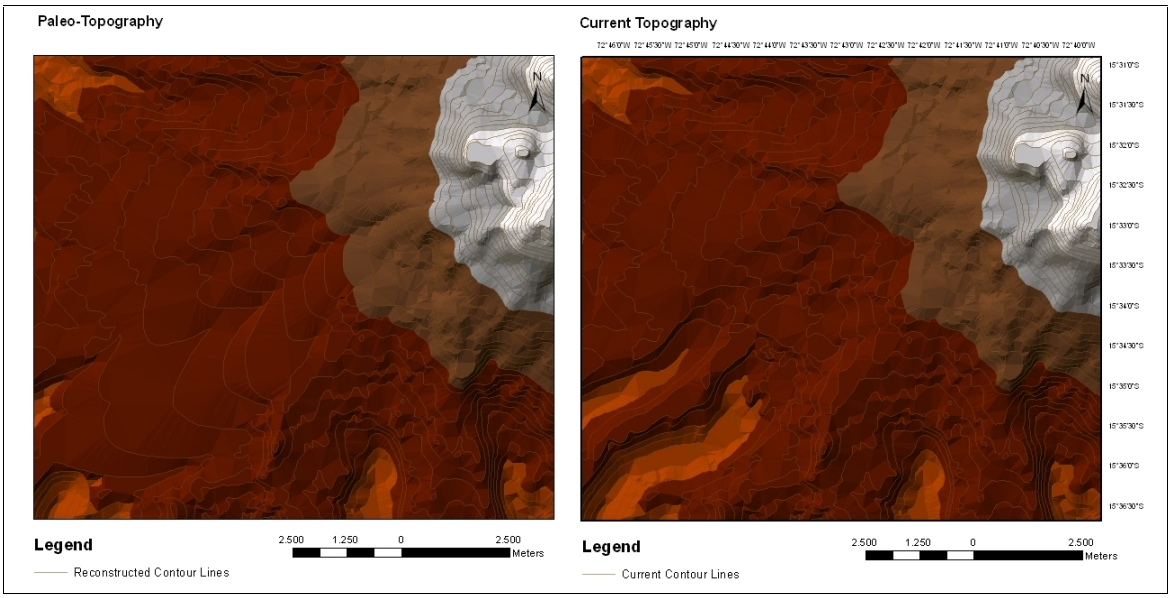

Figure 3. 5. Reconstructions of the topography for the paleo-ELA calculation compared with the actual topography

The spreadsheet calculate first the ELA AA, and then is weighted by different values of balance ratio (BR), the BR with the lowest standard deviation indicates the ELA with the best statistical probability of being correct (see chapter 2). The tables 3.2, 3.3 and 3.4 present the AABR calculations for 1955, 2007 and LLGM glacial phases. The selected ELAs values are highlighted in blue.

Table 3.2. AABR calculations for 1955.

QUEBRADA TUIALQUI	BR=1	BR=1,5	BR=2,0	BR=2,5	BR=3
Tuialqui 1	5672	5678	5714	5740	5761
Tuialqui 2	5812	5815	5833	5846	5855
Tuialqui 3	5634	5608	5636	5655	5669
Tuialqui 4	5829	5812	5840	5859	5874
Tuialqui 5	5556	5569	5585	5595	5603
Tuialqui 6	5724	5713	5738	5756	5769
MEAN	5705	5699	5724	5742	5755
STANDARD DEVIATION	105	102	103	104	105
QUEBRADA RIO BLANCO	BR=1	BR=1,5	BR=2,0	BR=2,5	BR=3
Rio Blanco 1	5988	5952	5971	5988	6001
Rio Blanco 2	5858	5880	5907	5926	5940
Rio Blanco 3	5704	5720	5736	5747	5756
MEAN	5850	5851	5871	5887	5899
STANDARD DEVIATION	142	119	121	125	128
QUEBRADA AZUFRIOC	BR=1	BR=1,5	BR=2,0	BR=2,5	BR=3
Azufrioc 1	5776	5752	5764	5775	5785
Azufrioc 2	6013	6000	6007	6013	6018
MEAN	5895	5876	5886	5894	5902
STANDARD DEVIATION	168	175	172	168	165
GENERAL SW SLOPE	BR=1	BR=1,5	BR=2,0	BR=2,5	BR=3
MEAN	5779	5773	5794	5809	5821
STANDARD DEVIATION	141	135	132	132	131

Table 3.3. AABR calculations for 2007.

QUEBRADA TUIALQUI	BR=1	BR=1,5	BR=2,0	BR=2,5	BR=3
Tuialqui 1	5746	5706	5723	5746	5764
Tuialqui 2	5819	5807	5825	5838	5847
Tuialqui 3	5700	5739	5763	5779	5791
Tuialqui 4	5889	5852	5872	5890	5903
Tuialqui 5	5579	5560	5552	5561	5568
Tuialqui 6	5814	5819	5841	5857	5868
MEAN	5758	5747	5763	5779	5790
STANDARD DEVIATION	109	106	117	119	120
QUEBRADA RIO BLANCO	BR=1	BR=1,5	BR=2,0	BR=2,5	BR=3
Rio Blanco 1	6102	6128	6150	6165	6177
Rio Blanco 2	5906	5930	5955	5973	5986
Rio Blanco 3	5767	5753	5768	5777	5785
MEAN	5925	5937	5958	5972	5983
STANDARD DEVIATION	168	188	191	194	196
QUEBRADA AZUFRIOC	BR=1	BR=1,5	BR=2,0	BR=2,5	BR=3
Azufrioc 1	5825	5804	5810	5820	5828
Azufrioc 2	6026	6015	6007	6002	6002
MEAN	5926	5910	5909	5911	5915
STANDARD DEVIATION	142	149	139	129	123
GENERAL SW SLOPE	BR=1	BR=1,5	BR=2,0	BR=2,5	BR=3
MEAN	5834	5828	5842	5855	5865
STANDARD DEVIATION	146	154	157	156	156

Table 3.4. AABR calculations for LLGM.

GENERAL SW SLOPE	BR=1	BR=1,5	BR=2,0	BR=2,5	BR=3
Paleo-glacier 1	4867	4872	4895	4911	4921
Paleo-glacier 2	4832	4800	4820	4834	4843
MEAN	4850	4836	4858	4873	4882
STANDARD DEVIATION	25	51	53	54	55

Figure 3.6 shows the altitude values of ELA in LLGM, 1955 and 2007 glacial phases, and the figure 3.7 presents the vertical shift in ELAs (ΔELA). The altitude has shifted 984 m from LLGM to 2007 and 13 m from 1955 to 2007, that means a vertical shift of 0,25 m/year.

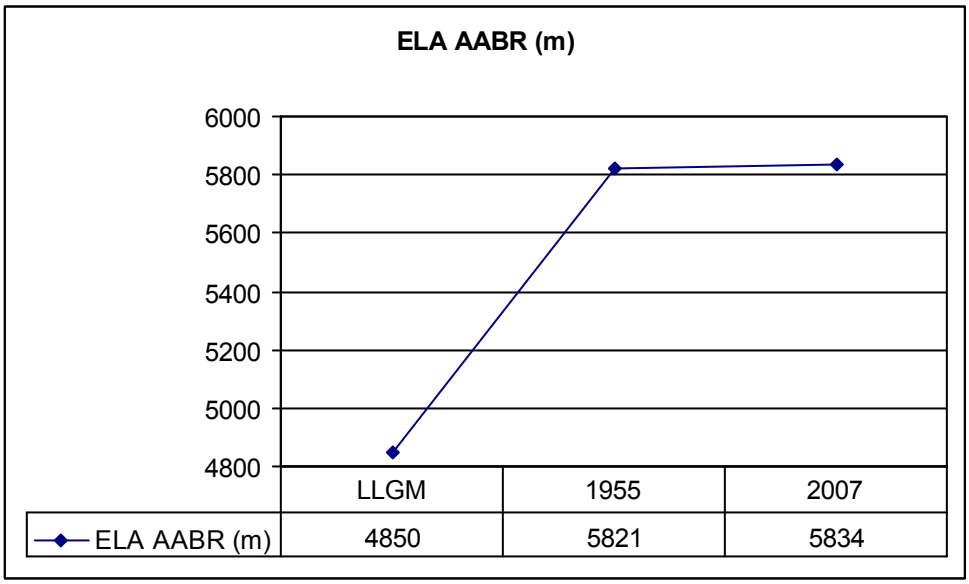

Figure 3. 6. Altitude values of ELA in LLGM, 1955 and 2007 glacial phases.

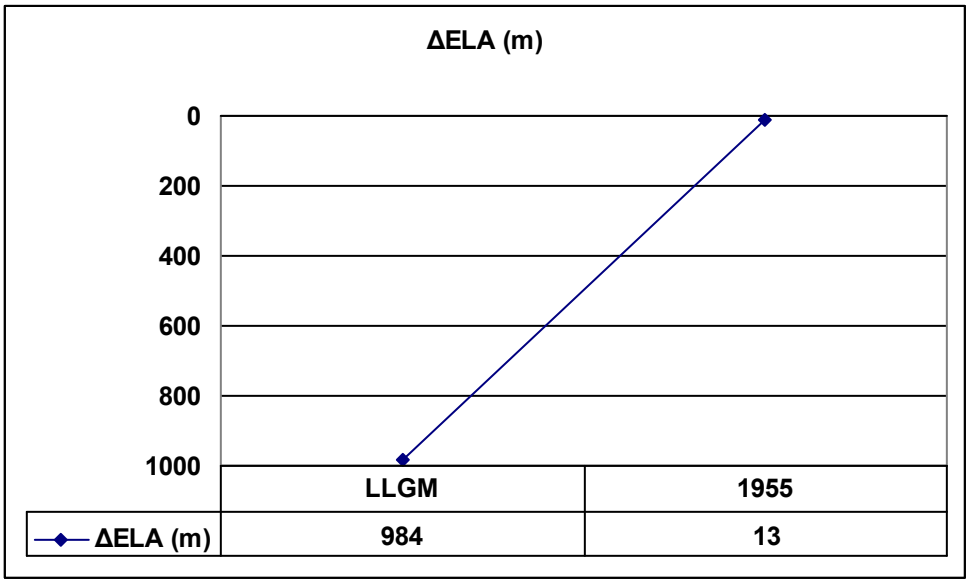

Figure 3. 7. Vertical shift in ELAs (ΔELA)

The results show an ELA vertical shift of 984 m from LLGM to 2007, and 13 m from 1955 to 2007. The changes in ELA are caused by changes in temperatures and climatic conditions, therefore is important the study of ELAs for the information that provides about the climate change.

3.4 Spatial model of ELAs and accumulation and ablation zones

As commented in chapter 2, the ELA is an imaginary line that separates the ablation zone and the accumulation zone. At this altitude, the amount of new snow gained by accumulation is equal to the amount of ice lost through ablation. In figure 3.8 and figure 3.9 the ELAs were plotted over the Google Earth mosaic, the figure shows that the modern ELA is still far of the upper limits of the glaciers, this would mean that the glaciers would disappear, because the non existence of the accumulation zone and the melting of the ice in the ablation zone.

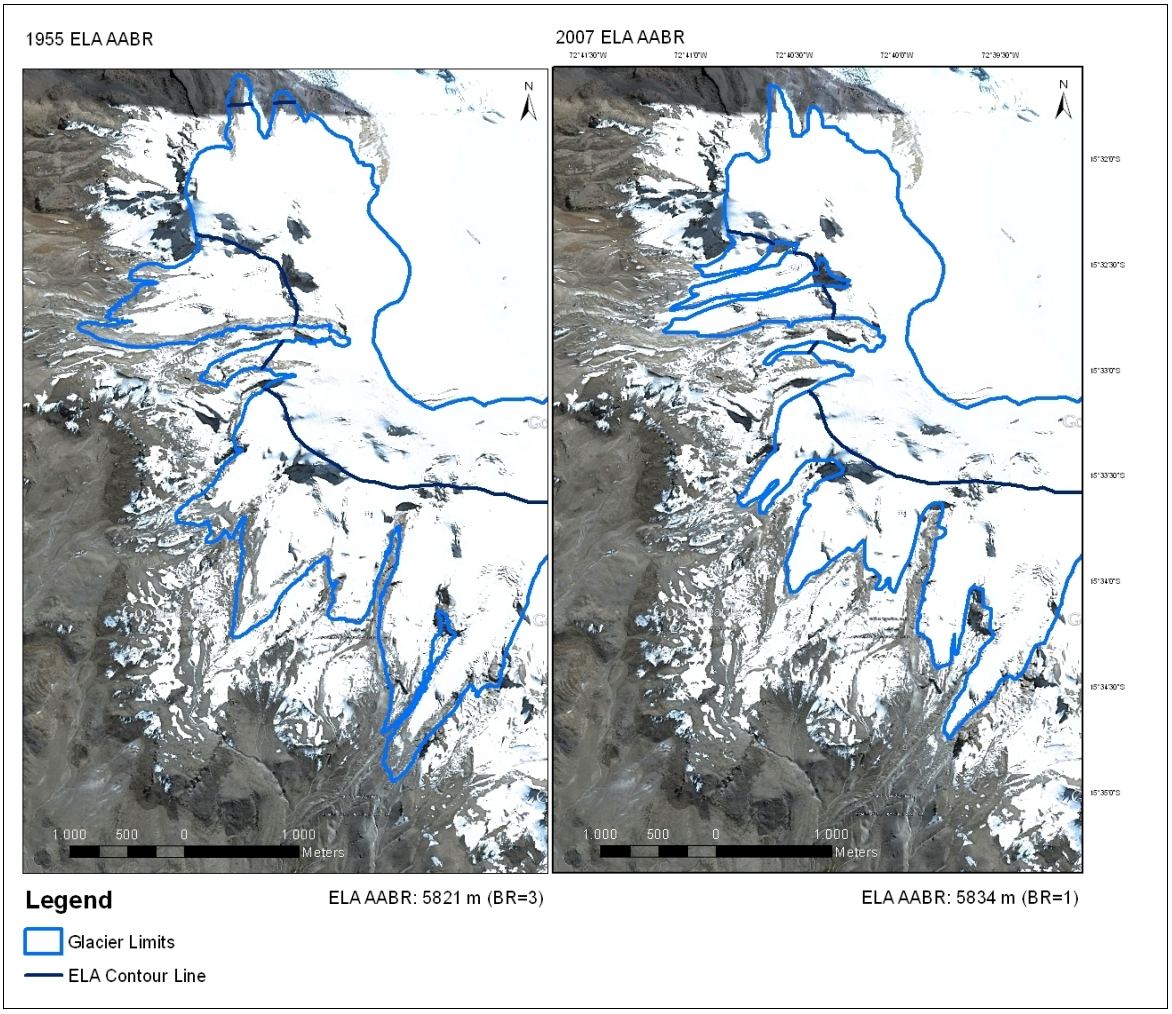

Figure 3. 8. 1955 and 2007 ELAs over the google earth mosaic

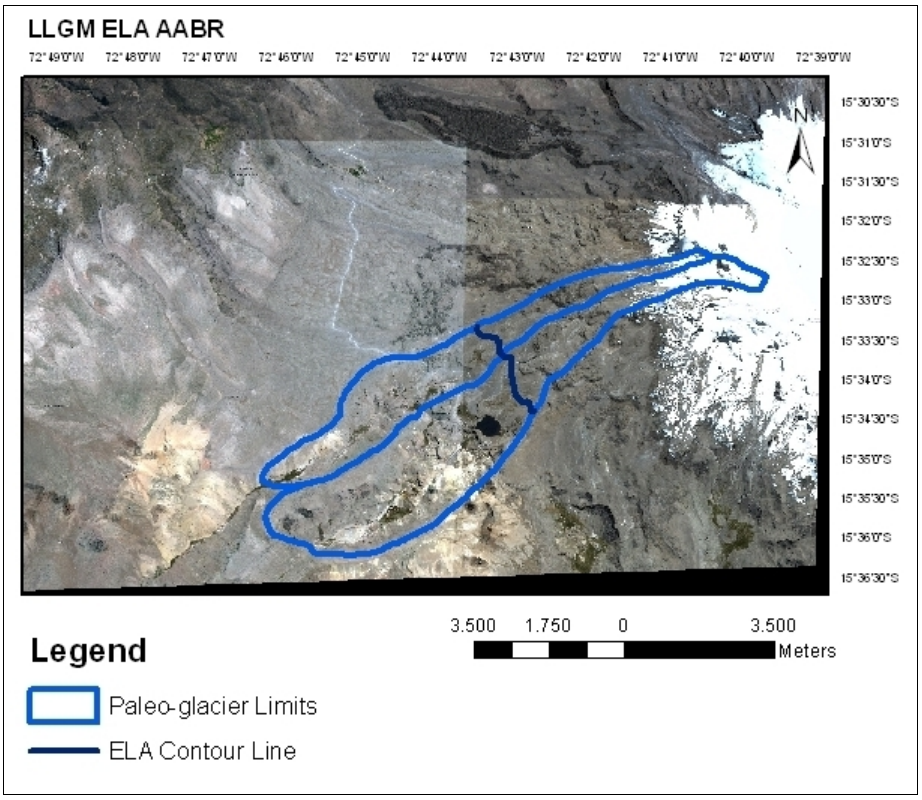

Figure 3. 9. LLGM paleo-ELAs over the google earth mosaic

Both accumulation and ablation surfaces has been decreased due to the glaciers retreat. The table 3.5 shows the accumulation and ablation surfaces in the 1955 and 2007 glacial phases. Figure 11 presents the data respect the total surface of the glaciers. The accumulation area has decreased from 5,02 km^2 in 1955 to 4,5 km^2 in 2007 (10,36%), and the ablation area also has decreased from 5,76 km^2 in 1955 to 3,9 km^2 in 2007 (31,22%).

Table 3.5. Accumulation and ablation surfaces in the 1955 and 2007 glacial phases.

	1955	2007	% total 1955	% total 2007
Accumulation	5,02	4,5	46,92	53,57
Ablation	5,67	3,9	52,99	46,43
TOTAL:	10,7	8,4		

These data explains that the percentage over the total surface has decreased in both accumulation and ablation zones, but percentage is higher in the ablation zone, this could mean that the ice in the ablation zone is melting quickly during the last years. The AAR (Accumulation Area Ratio) is the ratio of the accumulation area to the total glacier area: AAR = AC/TS, where AC is the accumulation area and TS is the total surface, this indicator has increased from 0,47 in 1955 to 0,54 in 2007. This indicates that the glaciers in 1955 had larger ablation area and in 2007 had a larger accumulation area. Is possible to follow the evolution using the mapped paleo-glacier, this glacier had larger ablation zone, 71,67% of the glacier (28,33% accumulation

zone), and their AAR was 0,28. Observing these results the trend seams clear, the percentage of the accumulation area is growing each glacier phase.

Is possible to study the variation of the climate analyzing the ELAs vertical shifts, because the changes in these vertical shifts are caused by changes in temperatures. An equation which assumes that changes in ELA are entirely a function of the changes in temperature was used by Úbeda (2010), this equation calculates the temperature shift from the product of the MALR (Moist Adiabatic Lapse Rate) and the shift in the ELA.

$$\Delta T = MALR * \Delta ELA$$

The vertical shift in ELA selected was the LLGM with respect to 2007, which is 984 m. According to Úbeda (2010) the MALR is 6,5ºC/km (0,0065ºC/m), and the MALR in the NE slope of Nevado Coropuna is 0,0084ºC/m, this last one was selected because of the geographic situation of the study area, this data is provided by a group of data loggers situated in NE slope of Coropuna since 2007. This MALR is close to the MALR dry limit of 0,0098ºC/m (Kaser & Osmaston 2002). This equation gives a temperature shift of 8,26 ºC (0,0082ºC/m) from LLGM to 2007 for the SW slope of Nevado Coropuna.

In summary, the ELAs can be provide valuable paleoclimatic information and could indicate the climatic trend for future predictions.

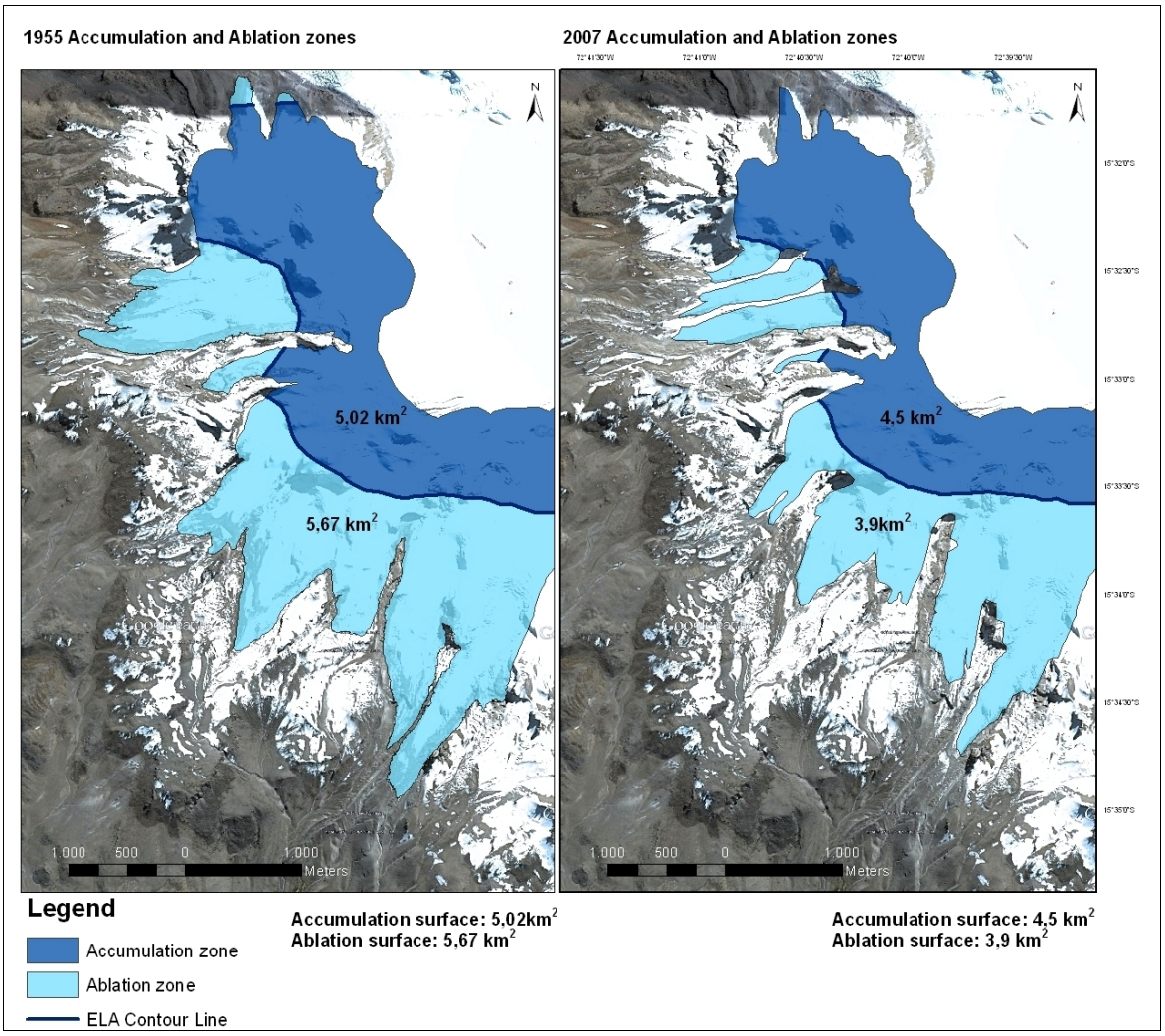

Figure 3. 10. Accumulation and ablation surfaces in 1955 and 2007

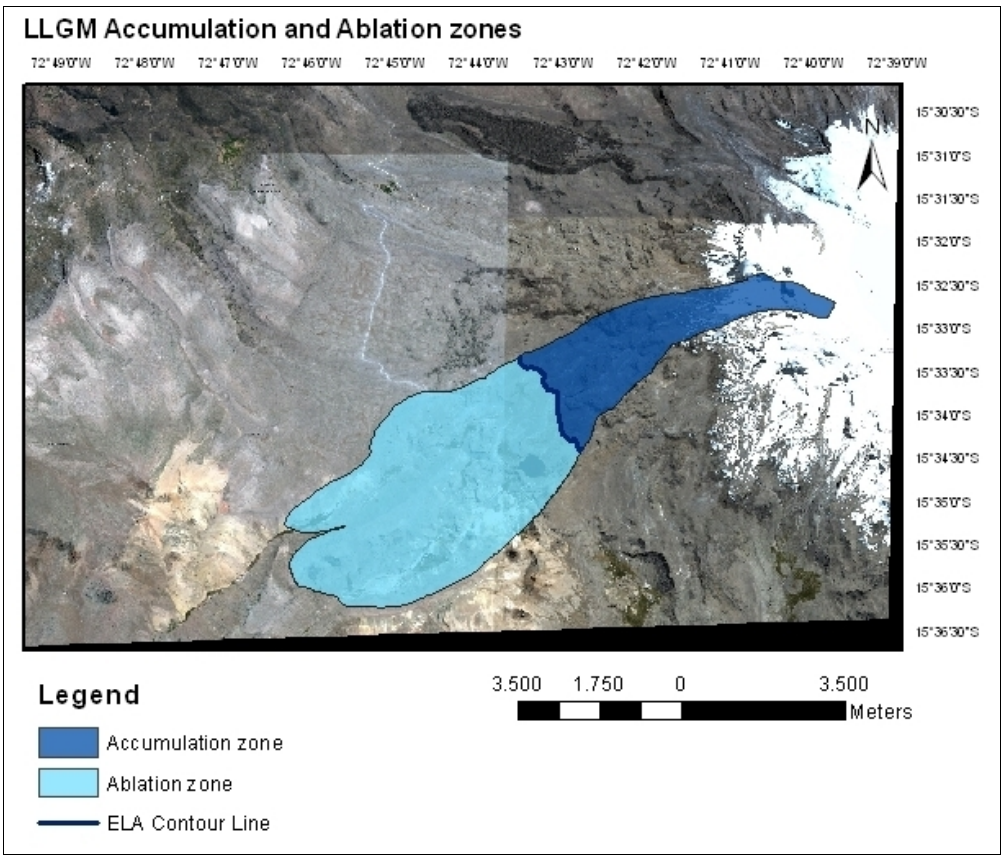

Figure 3. 11. Accumulation and ablation zones in LLGM paleo-glaciers.

CHAPTER 4

DISCUSSION AND FUTURE WORK

Glaciers of the tropical Andes are sensitive climate indicators because of their peculiar mass balance seasonality (Kaser and Osmaston, 2002). These glaciers exist only under certain conditions of temperature, precipitation and solar radiation receipt (Seltzer, 2001). The aim of this project was to reconstruct glacial phases in the SW slope of Nevado Coropuna in order to achieve valuable information of all the changes happened in the zone, analyze the glacier evolution and their relationship with the climate.

The results of the present work shows that the glaciated surface area has retreated 21,50% from 1955 to 2007, that means that in 2007 had the 78,50% of the glaciated area of 1955, from 10,7 km^2 to 8,4 km2, this is a deglaciation rate of 0,044 km^2/year. The ELA AABR vertical shift referred to 2007 was 13m for 1955 and 984 m for LLGM calculated glaciers, that means a vertical shift of 0,25 m/year from 1955 to 2007.

4.1 Moraine mapping

The moraine mapping is an important step in the process of paleo-glacier reconstruction establishing the geometry because geomorphological traces left by ancient glaciations (Giraldez, 2011). The moraine mapping I used in this analysis has been done previously by GFAM-GEM through photointerpretation techniques using a stereoscope with aerial photographs and Google Earth images in the interpretation process. The mapped moraines from LLGM were between 4450 and 4700 m.

Alcala et al. (2011) suggest that on Ampato volcanic complex the ice tongues reached a minimum elevation of 4270 m during the LGMA, with a minimum on the southern side (4240 m). During the most important re-advance phase the glacier front was at 4520 m, as shown by the moraine record. On Sabacaya, the moraine record was largely covered by recent lava flows, except in one of the valleys of the western side, where the moraines show a minimum altitude of 4430 m for the LGMA. In the present investigation, LLGM moraines in SW slope of Nevado Coropuna were higher than those studies, this differences probably are given by the using of different dating methods or differences related to the glacier locations and topography.

According to Smith et al.(2005c), in some regions the glacial advances of the local LGM are relatively minor compared to older advances, differences in valley hypsometry and maximum peak altitudes seem likely to have played a role in these regional variations. For several authors (e.g. Rodbell and Seltzer, 2000) there is no solid evidences for glacial advances in the tropical Andes during the YD climate reversal.

(Robell et al., 2009) suggest that there was a significant ice re-advance at the onset of YD because a well-dated moraines, however, ice was retreating during much of the remaining YD interval. Also suggested that the spatial–temporal pattern of Holocene glaciation exhibits tantalizing but incomplete evidence for an Early to Mid-Holocene ice advance in many regions, but not in the arid subtropical Andes, where moraines deposited during or slightly prior to the Little Ice Age (LIA) record the most extensive advance of the Holocene. And Licciardi et al.(2009) do not exclude the possibility of multiple Holocene glacier expansions. However, the combined geomorphic and geochronologic evidence clearly indicates the dominance of two major episodes,

including an early Holocene glacial interval and a somewhat less extensive glaciation during the LIA.

Some authors suggest different dating of the YD moraines, from these different ideas can be deduced that these moraines may need further study.

Úbeda (2010) classified the moraines of the Nevado Coropuna volcanic complex in four big groups, depending to their relative chronologies:
(1): Last advance, during LIA, between XVI and XIX century.
(2): Re-advance later to the LLGM
(3): Last maximum advance, in the LLGM, between 22 and 12 ka.
(4): Advances and re-advances earlier to the LLGM

Summarizing, the moraine mapping of the study zone showed in this work is based on Úbeda (2010) mapping shows the altitude of moraines in LLGM, Holocene and LIA glacial phases. As I said before the differences with other studies probably are given by the using of different dating methods or differences related to the glacier locations and topography.

4.2 Glacier delimitation and surface calculation

For the reconstruction of the climate history, the delimitation of the glaciers and paleo-glaciers is very important due to the clues that they bring through the reconstruction of their ELAs and surfaces. Photographs from aerial flights and satellite images were used to delimit current glaciers, and the moraine mapping to delimit paleo-glaciers.

The results obtained shows that the 1955 glacier limits were from 5050 m the lower glacier limit (Tuialqui 1) and the upper glacier limit 6350 m (Rio Blanco 1), the 2007 limits for the same glaciers were 5150 m and 6350 m respectively. The glaciated area has been retreated in all the glaciers of the zone of study, the total glaciated surface was 10,7 km^2 in 1955 and 8,4 km^2 in 2007, this means a 21,5% retreat of the total glaciated surface in 1955. Individually the Tuialqui 5 glacier are retreat with 46,39% and Tuialqui 2 only loss 2,56% of their glaciated area.

Racovietanu et al. (2007) suggested a reduction of the ice cover of approximately 26% between 1962 and 2000 on Nevado Coropuna. Úbeda and Palacios (2009) calculated a reduction of the glacial system surface for the entire Nevado Coropuna of ~18% in 52 years (from 1955 to 2007). They pointed that the process appears to have speeded up in the last decades (~13% in only 21 years). These results are similar to those obtained in the chapter 3, a 21,5% retreat between 1955 and 2007.

Giraldez (2011) obtained in the SW slope of Nevado Hualcán a deglaciation rate of 0,076 km^2/year, while in the present work the deglaciation rate was 0,044 km^2/year, the differences in this case seems to be the glacier locations and the different topography.

In summary, the glacier delimitation helps to calculate the surface of the glaciers and offers quantitative information of their evolution. Due to the tropical glaciers are sensitive indicators of climate change, their delimitation can help to study the evolution of the glaciers and predict the future of the resources that they provide to the population around.

4.3 ELAs AABR

Paleo-climatic reconstructions based on the limits of former glaciers commonly make use of estimates of the associated equilibrium-line altitudes (ELAs), where accumulation of snow is exactly balanced by ablation. The equality of accumulation and ablation at the ELA means that the local climate can be parameterized in terms of accumulation-season precipitation and ablation-season temperatures, using statistical and analytic methods (Kuhn, 1989; Ohmura et al, 1992; Selzer, 1994).

I the present study I calculated the ELAs of the SW slope of Nevado Coropuna following the AABR method (Area x Altitude Balance Ratio). The results show ELA AABR altitudes of 5821 m for 1955 and 5834 m for 2007, with an altitude shift of 13 m, to further study in this concrete point a field work would be required, but that was out of the scope of the present work. I calculated also the paleo-ELA of a paleo-glacier of the zone of study obtaining a result of 4850 m, which can be an indicator of the approximate paleo-ELA of the zone of study in LLGM.

The results I have obtained can be compared with Úbeda (2010) investigation in the Coropuna volcanic complex. This author found that the altitude of the ELA AABR in the SE slope was 5844 m for 2007, similar to the result in the present work that suggests an ELA AABR of 5834 for 2007 in the SW slope. However the vertical shift is lower in the present work, this could be because of the different topography of both slopes, a future research will be required for specify this point.

According with Giráldez (2011), Kaser and Osmaston (2002) considered the value AAR=0,67 as the most appropiate for tropical glaciers. In their investigation, Úbeda (2010) obtained a mean AAR value of 0,58 for the flaciers in the Coropuna volcanic complex and Giráldez (2011) found a range from 0,54 in YD to 0,51 in 2003 in the study of the SW slope of Nevado Hualcán. In the present study, the obtained value was 0,54 in 2007 for the SW slope of Nevado Coropuna, close to the results of the mentioned authors.

A common approach to investigating the structure of past climate events is to reconstruct paleo-snowlines (frequently equated with the ELA) on glaciated or formerly glaciated peaks, as a proxy for mean atmospheric temperature (Benn et al., 2005).

Bromley et al. (2011) calculated the modern ELAs for Coropuna's glaciers obtaining an average results of 5850 ± 54 m for the West slope and 5580 ± 54 m for South aspect. In the present study the mean obtained value was 5834 m, this is closest to the W slope results of Bromley, this could be because the geographic position of the analyzed glaciers (more in the West than in South). According to (Benn et al., 2005) the altitude of the equilibrium line is rarely constant across a glacier, but varies with patterns of snow accumulation, shading, and other factors.

Alcalá et al. (2011) reported an LLGM ELA in the Huayuray valley of 4980 m. Bromley et al. (2001) used the MELM (Maximum Elevation of Lateral Moraines) and THAR (Terminus Headwall Altitude Ratio) methods for the calculation of LLGM ELAs for the Puncuncho peaks, the results reported with the MELM method were an average of 4887 ± 77 m for the W slope and 4745 ± 66 m for the S, and with the THAR method (with ratio of 0,28), an avegare of 5059 ± 68 m for West and 4728 ± 228 for the South. ELA values are highest on northflowing glaciers and lowest on south-flowing glaciers. The ELA ABR for LLGM obtained in the present study was 4850 m, this result is close to the reported by Bromley et al. (2001) with the MELM method.

Changes in ELAs are caused by changes in climatic conditions, this climatic interpretations can be studied based on ELAs with different methods, and allow to understanding that changes and their implication. Analyzing the ELAs vertical shift is possible to study the climate change, the changes in temperature was estimated multiplying the MALR and the ΔELA. The results obtained was a ΔT of 8,26 ºC/km (0,0082ºC/m) from LLGM to 2007 for the SW slope of Coropuna. These results are very close to Úbeda (2010) study for the NE slope of Coropuna.

4.4 Conclusions

Glaciers not only reveal information about climate change, they are very important as a water supply for the population who is living around, and they can cause natural hazards. The investigation and monitoring of the glaciers makes them valuable for climate research, and their future evolution can be predicted.

The aim of this project was to reconstruct the glacial phases in the SW slope of Nevado Coropuna in order to generate quantitative information of surface areas and ELAs as a first step for the analysis of glacier evolution and the achievement of valuable information of the changes that have happened.

The specific conclusions of the present study are:

(1): Moraines on the SW slope of Nevado Coropuna served as the reference to reconstruct the geometry of paleo-glaciers in LLGM glacial phase. Modern glaciers from 1955 and 2007 were also delimited using aerial photographs for 1955 glaciers and Google Earth image mosaic for 2007 glaciers.

(2): The surface areas of the glaciers were calculated from their delimitation. The results indicated that the total surface has retreated 2,3 km^2 from 1955 to 2007, this is a reduction of the 21,5% of the glaciated surface. The deglaciation rate is 0,044 km^2/year (44.000 m^2/year).

(3): The ELAs AABR of the glaciers were calculated from their delimitation. The results show an altitudinal shift of the ELA of 13 m from 1955 to 2007 and 984 m from LLGM to 2007. The analysis shows ELA AABR altitudes of 5834 m for actual glaciers (2007), this data match with the results of other authors.

(4): Is assumed that ELAs vertical shifts are caused by changes in temperatures. By analyzing the ELAs vertical shift is possible to study the climate change. The temperature shift from LLGM to 2007 in the NW slope of Nevado Coropuna was 8,26ºC/km (0,0082ºC/m).

REFERENCES

Alcalá, J., Palacios, D., Zamorano, J.J. and Vázquez-Selem, L. (2011). Last Glacial Maximum and deglaciation of Ampato volcanic complex, Southern Peru. Rev. C. & G., 25 (1-2), 121-136.

Allmendinger, R.W., Jordan, T.E., Kay, S.M., Isacks, B.L., (1997). The evolution of the Altiplano-Puna Plateau of the central Andes. Annual Review Earth and Planetary Science 25, 139–174.

Ammann C, Jenny B, Kammer K, Messerli B. (2001). Late Quaternary glacier response to humidity changes in the arid Andes of Chile (18–29- S). Palaeogeography, Palaeoclimatology, Palaeoecology 172: 313–326.

Anders MH, Gregory-Wodzicki KM, Spiegelman M. (2002). A critical evaluation of late Tertiary accelerated uplift rates for the Eastern Cordillera, Central Andes of Bolivia. Journal of Geology 110: 89–100.

Ballantyne, C.K., (2002). Paraglacial geomorphology. Quaternary Science Reviews 21, 1935–2017.

Benn, D.I., Gemmell, A.M.D. (1997). Calculating equilibrium-line altitudes of former glaciers by the balance ratio method: a new computer spreadsheet Glacial Geology and Geomorphology.

Benn, D. I., Owen, L. A., Osmaston, H. A., Seltzer, G. O., Porterd, S. C. and Mark, B. (2005). Reconstruction of equilibrium-line altitudes for tropical and sub-tropical glaciers. Quaternary International 138–139, 8–21.

Bromley G.R.M., Schaefer J.M., Winckler, G., Hall, B.L., Todd, C.E. & Rademaker D.K. M. (2009). Relative timing of last glacial maximum and late-glacial events in the central tropical Andes. Quaternary Science Reviews, 28, 2514-2526.

Bromley G.R.M., Hall, B.L., Schaefer J.M., Winckler, G., Todd, C.E. and Rademaker (2010). Glacier fluctuations in the southern Peruvian Andes during the late-glacial period, constrained with cosmogenic 3He.Journal of Quaternary Science (2011) 26(1) 37–43.

Bromley G.R.M,, Hall, B.L., Rademaker, K.M., Todd, C.E. and Racovteanu, A.E. (2011). Late Pleistocene snowline fluctuations at Nevado Coropuna (15ºS), southern Peruvian Andes. Journal of Quaternary Science. DOI: 10.1002/jqs.1455.

Clapperton CM. (1993). Quaternary Geology and Geomorphology of South America. Elsevier: Amsterdam.

Dewey JF, Lamb SH. (1992). Active tectonics in the Andes. Tectonophysics 205: 79–95.

Dornbusch, U. (1997). Geomorphologische Untersuchungen zur jungquartären Vergletscherung der Westanden Südperus zwischen 14º25'S und 15º30'S, daraus ableitbare klimatische Bedingungen und deren Vergleich mit neu erarbeiteten Angaben zur rezenten Verteilung von Temperatur, Niederschlag und Schneegrenzhöhen in Südperu südlich 12ºS. Diss. Freie Universität Berlin, 185 pp.

Dornbusch U. (1998). Current large-scale climatic conditions in southern Peru and their influence on snowline altitudes. Erdkunde 52: 41–54.

Dornbush, U. (2000). Pleistocene glaciation of the dry western Cordillera in Southern Peru (14º25'-15º30' South). Glacial Geology and Geomorphology.

Farber DL, Hancock GS, Finkel RC, Rodbell D. 2005. The age and extent of tropical alpine glaciation in the Cordillera Blanca, Peru. Journal of Quaternary Science 20: 759– 776.

Dornbusch, U. (2002). Pleistocene and present day snowlines rise in the Cordillera Ampato, Western Cordillera, southern Peru (14º25'-15º30' South). Neues Jahbuch für Geologie und Palaeontologie Abhandlungen, 225, 103-126.

Fell, R. (1994). Landslide risk assessment and acceptable risk. Canadian Geotechnical Journal 31:261–72.

Garreaud R, Vuille M, Clement AC. (2003). The climate of the Altiplano: observed current conditions and mechanisms of past changes. Palaeogeography, Palaeoclimatology, Palaeoecology 194: 5–22.

GFAM-GEM. Cartografía geomorfológica del complejo volcánico Nevado Coropuna (cordillera occidental de los Andes Centrales, sur de Perú)

Giráldez, C. (2011). Glacier evolution in the South West slope of Nevado Hualcán (Cordillera Blanca, Perú). Master Thesis. Universidad Complutense de Madrid

Glaciers of South America, (1998). United States Geological Survey Professional Paper 1386-I.

Glasser, N. F., Clemmens, S., Schnabel, C., Fenton, C. R. and McHargue, L. (2009). Tropical glacier fluctuations in the Cordillera Blanca, Peru between 12.5 and 7.6 ka from cosmogenic 10Be dating. Quaternary Science Reviews, 28, 3448–3458.

Goodman AY, Rodbell DT, Seltzer GO, Mark BG. (2001). Subdivision of glacial deposits in southeastern Peru based on pedogenic development and radiometric ages. Quaternary Research 56: 31–50.

Greminger, P. (2003). Managing the risks of natural hazards. In Debris-fl ow hazards mitigation: Mechanics, prediction, and assessment: Proceedings, 3rd International DFHM Conference, Davos, Switzerland, September 10–12, 2003, ed. D. Rickenmann and C. L. Chen, 39–56. Rotterdam: Millpress.

Gubbels TL, Isacks BL, Farrar E. (1993). High-level surfaces, plateau uplift, and foreland development, Bolivian central Andes. Geology 21: 695–698.

Guilderson, T.P., Fairbanks, R.G., Rubenstone, J.L., (1994). Tropical temperature variations since 20,000 years ago: modulating interhemispheric climate change. Science 263, 663–665.

Habereli, W. (2010): Glaciers in an environmental context Part 1: Paleoglaciology. Department of Geography, University of Zurich

Hall SR, Ramage JM, Rodbell DT, Finkel RC, Smith JA, Mark BG, Farber DL. (2006). Geochronology and equilibrium line altitudes of LLGM through Holocene glaciations from the tropical Cordillera Huayhuash, Peru (Abstract PP31C-1767). Eos (Transactions, American Geophysical Union), Fall Meeting Supplement 87 52.

Hastenrath, S. (2009). Past glaciation in the tropics. Quaternary Science Reviews, 28, 790-798.

Herreros, J., Moreno, I. , Taupin, J.-D. , Ginot, P., Patris, N., De Angelis, M., Ledru, M.-P., Delachaux, F. and Schotterer, U. (2009). Environmental records from temperate glacier ice on Nevado Coropuna saddle, southern Peru. Adv. Geosci., 22, 27–34.

Hoblitt, R.P.; Miller, C.D., and Scott, W.E. (1996). Volcanic Hazards with Regard to Siting Nuclear-Power Plants in the Pacific Northwest. U.S. Geological Survey Open-File Report 87-297.

Hostetler, S.W., Mix, A.C., (1999). Reassessment of ice-age cooling of the tropical ocean and atmosphere. Nature 399, 673–676.

Hostetler, S.W., Clark, P.U., (2000). Tropical climate at the Last Glacial Maximum inferred from glacier mass-balance modelling. Science 290, 1747–1750.

Huggel, C., Haeberli, W., Kääb, A., Bieri, D. and Richardson, S: (2004). An assessment procedure for glacial hazards in the Swiss Alps. Canadian Geotechnical Journal, 41, 1068-1083.

Huggel, C; Haeberli, W; Kääb, A (2008). Glacial hazards: perceiving and responding to threats in four world regions. In: Orlove, B [et al.]. Darkening Peaks: Glacier Retreat, Science, and Society. Berkeley, US, 68-80.

Isacks BL. (1988). Uplift of the central Andean plateau and bending of the Bolivian Orocline. Journal of Geophysical Research 93: 3211– 3231.

Johnson AM. (1976). Climate of Peru, Bolivia, and Ecuador. In World Survey of Climatology, Vol. 12, Schwerdtfeger W, (ed.). Elsevier: New York; 147–218.

Jordan TE, Isacks BL, Allmendinger RW, Brewer JA, Ramos VA, Ando CJ. (1983). Andean tectonics related to geometry of subducted Nazca plate. Geological Society of America Bulletin 94: 341–361.

Kaser, G., (1995). Some notes on the behaviour of tropical glaciers. Bull. Inst. Fr. Etudes Andines 24 _3., 671–681.

Kaser, G., (1996). Gletscher in den Tropen- ein Beitrag zur Geographie der tropischen Hochgebirge. Habilitationsschrift, Universit¨at Innsbruck.

Kaser, G., (1998). The Nature of Tropical Glaciers. International Hydrological Series. UNESCO-Cambridge Univ. Press _accepted and in preparation.. English version of:

Kaser, G., (1999). A review of the modern fluctuations of tropical glaciers. Global and Planetary Change 22, 93–103.

Kaser G. (2001). Glacier–climate interaction at low latitudes. Journal of Glaciology 47: 195–204.

Kaser G, Osmaston H. (2002). Tropical Glaciers. Cambridge University Press: Cambridge, UK.

Kaser, G. & Osmaston, H., (2002). Tropical Glaciers. International Hydrology Series. Cambridge University Press, Cambridge (U.K.), 207 pp.

Kelly MA, Thompson LG. (2004). 10Be dating of late-glacial moraines near the Cordillera Vilcanota and the Quelccaya Ice Cap, Peru (Abstract PP23A-1388). Eos (Transactions, American Geophysical Union), Fall Meeting Supplement 85 47.

Kennan L. (2000). Large-scale geomorphology of the Andes; interrelationships of tectonics, magmatism and climate. In Geomorphology and Global Tectonics, Summerfield MA, (ed.). Wiley: Chichester; 167–199.

Kessler A, Monheim F. (1968). Der Wasserhaushalt des Titicacasees nach neueren Messergebnissen. Erdkunde 22: 275–283.

Klein, A.G. & Isacks, B.L. (1998). Alpine glacial geomorphological studies inthe Central Andes using Landsat Thematic Mapper images. Glacial Geology and Geomorrphology, rp01/1998.

Kley J. (1999). Geologic and geometric constraints on a kinematic model of the Bolivian Orocline. Journal of South American Earth Sciences 12: 221–235.

Kuhn, M. (1989). The response of the equilibrium line altitude to climate fluctuations: theory and observations. In: Oerlemans, J. (Ed.), Glacier Fluctuations and Climate Change, Kluwer, Dordrecht, 407-417.

Lal D. (1991). Cosmic ray labeling of erosion surfaces: in situ nuclide production rates and erosion models. Earth and Planetary Science Letters 104: 424–439.

Lamadon S. (1999).- Fluctuations glaciaires et téphrostratigraphie dans les montagnes intertropicales : une revue et applications dans les Andes du Sud du Pérou (massifs des Nevados Ampato et Coropuna). Mémoire DEA, Université Blaise Pascal, Clermont-Ferrand, 205 p.

Licciardi, J.M., Schaefer, J.M., Taggart, J.R. and Lund, D.C. (2009). Holocene Glacier Fluctuations in the Peruvian Andes Indicate Northern Climate Linkages. Science 325, 1677.

Lifton NA, Bieber JW, Clem JM, Duldig ML, Evenson P, Humble JE, Pyle R. (2005). Addressing solar modulation and long-term uncertainties in scaling secondary cosmic rays for in situ cosmogenic nuclide applications. Earth and Planetary Science Letters 239: 140–161.

Mark BG, Seltzer GO, Rodbell DT, Goodman AY. (2002). Rates of deglaciation during the last glaciation and Holocene in the Cordillera Vilcanota-Quelccaya Ice Cap region, southeastern Peru. Quaternary Research 57: 287–298.

Mark, B.G., (2008). Tracing tropical Andean glaciers over space and time: Some lessons and transdisciplinary implications. Global and Planetary Change 60 (2008) 101–114

Mercer JH, Palacios MO. (1977). Radiocarbon dating of the last glaciation in Peru. Geology 5: 600–604.

Mercer JH. (1982). The last glacial–deglacial hemicycle in Peru. American Quaternary Association Conference Abstracts 7: 139.

Mercer JH. (1984). Late Cainozoic glacial variations in South America south of the

equator. In Late Cainozoic Palaeoclimates of the Southern Hemisphere: Proceedings of an International Symposium Held by the South African Society for Quaternary Research, Swaziland, 29 August–2 September, 1983. A.A. Balkema: Rotterdam; 45–58.

Messerli, B., (2001). The International Year of Mountains (IYM), the Mountain Research Initiative (MRI) and PAGES. Editorial, Pages News 9 (3), 2.

Montgomery, D.R., Balco, G., Willett, S.D., (2001). Climate, tectonics, and the morphology of the Andes. Geology 29 (7), 579–582.

Ohmura, A., Kasser, P. and Funk, M. (1992). Climate at the equilibrium line of glaciers. Journal of Glaciology, 38, 397-411.

Osmaston, H.A. (2005). Estimates of glacier equilibrium line altitudes by the AreaxAltitude, the AreaxAltitude Balance Ratio and the AreaxAltitude Balance Index methods and their validation. Quaternary International, 138– 139, 22–31.

Paterson, W.S.B., 1994. The Physics of Glaciers, third ed. Pergamon, Oxford 480pp.

Plazcek C, Quade J, Patchett PJ. (2006). Geochronology and stratigraphy of late Pleistocene lake cycles on the southern Bolivian Altiplano: implications for causes of tropical climate change. GSA Bulletin 118: 515–532.

Racoviteanu, A.E., Manley, W., Arnaud, Y., Williams, M.W. (2007). Evaluating digital elevation models for glaciologic applications: an example from Nevado Coropuna, Peruvian Andes. Global and Planetary Change 59 (1–4), 110–125.

Rodbell, D.T. (1991). Late Quaternary glaciation and climatic change in the northern Peruvian Andes. Ph.D. Dissertation, University of Colorado, Boulder, Colorado, 216 pp.

Rodbell. D.T. (1992). Late Pleistocene equilibrium line reconstructions in the northern Peruvian Andes. Boreas, 21, 43-52.

Rodbell DT, Seltzer GO. (2000). Rapid ice margin fluctuations during the YD in the tropical Andes. Quaternary Research 54: 328–338.

Rodbell, D.T., Smith, J. A. and Mark, B.G. (2009). Glaciation in the Andes during the Lateglacial and Holocene. Quaternary Science Reviews. Quaternary Science Reviews 28 (2009) 2165–2212

Selzer, G.O. (1994). Climatic interpretation of alpine snowline variations on millenial timescales. Quaternary Research, 41: 154-159.

Seltzer G, Rodbell DT, Burns S. (2000). Isotopic evidence for late Quaternary climatic change in tropical South America. Geology 28: 35–38.

Seltzer GO. (2001). Late Quaternary glaciation in the tropics: future research directions. Quaternary Science Reviews 20: 1063–1066.

Seltzer GO, Rodbell DT, Baker PA, Fritz SC, Tapia PM, Rowe HD, Dunbar RB. (2002). Early warming of tropical South America at the last glacial–interglacial transition. Science 296: 1685–1686.

Seltzer, G.O., Rodbell, D.T., Baker, P.A., Fritz, S.C., Tapia, P.M., Rowe, H.D., Dunbar, R.B., (2002). Early warming of tropical South America at the Last Glacial–interglacial transition. Science 296, 1685–1686.

Sissons, J.B. (1974). A late glacial ice cap in the central Grampians, Scotland. Transactions of the Institute of British Geographers 62, 95–114.

Sissons, J.B., (1980). The Loch Lomond advance in the Lake District, northern England. Transactions Royal Society Edinburgh: Earth Sciences 71, 13–27.

Smith, J. A., Finkel, R. C., Farber, D. L., Rodbell, D. T. and Seltzer, G. O. (2005). Moraine preservation and boulder erosion in the tropical Andes: interpreting old surface exposure ages in glaciated valleys. J. Quaternary Sci., Vol. 20 pp. 735–758.

Smith JA, Seltzer GO, Farber DL, Rodbell DT, Finkel RC. (2005b) Early local last glacial maximum in the tropical Andes. Science 308: 678– 681.

Smith JA, Finkel RC, Farber DL, Rodbell DT, Seltzer GO. (2005c) Moraine preservation and boulder erosion in the tropical Andes: interpreting old surface exposure ages in glaciated valleys. Journal of Quaternary Science 20: 735–758.

Smith, J. A., Mark, B. G. and Rodbell, D. T. (2008). The timing and magnitude of mountain glaciation in the tropical Andes. J. Quaternary Sci., Vol. 23 pp. 609–634.

Solomina, O., Jomelli, V., Kaser, G., Ames, A., Berger, B. and Pouyaud, B. (2007). Lichenometry in the Cordillera Blanca, Peru: "Little Ice Age" moraine chronology. Global and Planetary Change 59 225–235.

Stern, C R. (2004). Active Andean volcanism: its geologic and tectonic setting. Department of Geological Sciences, University of Colorado, Boulder, Colorado, 80309-0399 U.S.A.

Stone JO. (2000). Air pressure and cosmogenic isotope production. Journal of Geophysical Research, B, Solid Earth and Planets 105: 23 753–23 759.
Tanguy, J.; et al. (1998). "Victims from volcanic eruptions: a revised database". Bulletin of Volcanology 60: 140.

Thompson, L.G., Mosley-Thompson, E., Brecher, H., Davis, M., Leon, B., Les, D., Lin, P.-N., Mashiotta, T., Mountain, K., (2006). Abrupt tropical climate change: past and present. Proceedings National Academy of Science 103 (28), 10536–10543.

Thouret, J.-C., Juvigne, E., Mariño, J., Moscol, M., Loutsch, I., Davila, J., Legeley-Padovani, A., Samadon, S.and Rivera, M. (2002). Late Pleistocene and Holocene tephro-stratigraphy and chronology in Southern Peru. Boletín de la Sociedad Geológica del Perú v. 93, p. 45-61

Úbeda, J. & Palacios D. (2009) Reconstruction of mass balance of Nevado Coropuna glaciers (Southern Peru) for Late Pleistocene, Little Ice Age and the present. Geophysical Research Abstracts, Vol. 11, EGU2009-7922-2

Úbeda, J., Palacios, D. & Vázquez, L. (2009). Reconstruction of Equilibrium Line Altitudes of Nevado Coropuna Glaciers (Southern Peru) from the Late Pleistocene to the present. Geophysical Research Abstracts, 11, EGU2009-8067-2

Úbeda, J. (2010). El impacto del cambio climático en los glaciares del complejo volcánico Nevado Coropuna (Cordillera Occidental de los Andes Centrales). Universidad Complutense de Madrid.

Úbeda, J., (2012). Reconstrucciones Paleoclimáticas deducidas de la geomorfología glaciar y registros de la Guadarrama Monitoring Network Initiative (GUMNET). Poster. Departamento de Análisis Geográfico Regional y Geografía Física. Universidad Complutense de Madrid.

USGS Volcano Hazards Program. (2007). Lahars and Their Effects. Archived from the original on 2007-08-24. Retrieved 2007-09-02.

Venturelli G, Fragipane M, Weibel M, Antiga, D. (1978). Trace element distribution in the Cainozoic lavas of Nevado Coropuna and Andagua Valley, Central Andes of southern Peru. Bulletin of Volcanology 41: 213–228.

Vuille M, Keimig F. (2004). Interannual variability of summertime convective cloudiness and precipitation in the central Andes derived from ISCCP-B3 data. Journal of Climate 17: 3334–3348.

Vuille, M., Francou , B., Wagnon, P., Juen, I., Kaser, G., Mark, B.G., Bradley, R.S. (2008). Climate change and tropical Andean glaciers: Past, present and future. Earth-Science Reviews 89 (2008) 79–96

Vuille, M., Kaser, G., Juen, I., (2008). Glacier mass balance variability in the Cordillera Blanca, Peru and its relationship with climate and the large-scale circulation. Global and Planetary Change 62 (1–2), 14–28.

Wagnon P, Ribstein P, Francou B, Pouyaud B. (1999). Annual cycle of energy balance of Zongo Glacier, Cordillera Real, Bolivia. Journal of Geophysical Research 104(D4): 3907–3923.

Weibel M, Frangipane-Gysel M, Hunziker JC. (1978). Ein Beitrag zur Vulkanologie Su¨d-Perus. Geologische Rundschau 67: 243–252.

Zech R, Kull C, Kubik PW, Veit H. (2007). LGM and Late Glacial glacier advances in the Cordillera Real and Cochabamba (Bolivia) deduced from 10Be surface exposure dating. Climate of the Past 3: 623– 635.

Zech, R., May, J.-H., Kull, C., Ilgner, J., Kubik, P. W. and Veit, H. (2008). Timing of the late Quaternary glaciation in the Andes from _15 to 408 S. J. Quaternary Sci., Vol. 23 pp. 635–647.

TABLE OF FIGURES

CHAPTER 1 INTRODUCTION

Figure 1. 1. Geographical setting or Cordillera Occidental 5
Figure 1. 2. The tropics and their delimitations..... 6
Figure 1. 3. Geomorphological cartography of Nevado Coropuna 7
Figure 1. 4. Map of the Andes showing the location of Coropuna 9
Figure 1. 5. Annual and monthly mean precipitation 10

CHAPTER 2 METHODOLOGY

Figure 2. 1. Images from 1955 flight and ASTER 2007. 17
Figure 2. 2. Google Earth mosaic provided by GFAM-GEM..... 17
Figure 2. 3. Moraine mapping over W slope of Nevado Coropuna 19
Figure 2. 4. Names given to glaciers over Google Earth mosaic..... 21
Figure 2. 5. 1955 Contour belt sections 24
Figure 2. 6. Attribute table with the selected contour belt..... 24

CHAPTER 3 RESULTS

Figure 3. 1. Moraine mapping of the zone of the paleo-glaciers..... 32
Figure 3. 2. 1955 and 2007 glacier limits over Google Earth image mosaic 33
Figure 3. 3. Comparison of the glaciated area in 1955 and 2007 34
Figure 3. 4. Comparison of the evolution of each glacier..... 35
Figure 3. 5. Reconstructions of the topography..... 36
Figure 3. 6. Altitude values of ELA in LLGM, 1955 and 2007 glacial phases. 39
Figure 3. 7. Vertical shift in ELAs (ΔELA)..... 39
Figure 3. 8. 1955 and 2007 ELAs over the Google Earth mosaic..... 40
Figure 3. 9. LLGM paleo-ELAs over the Google Earth mosaic..... 41
Figure 3. 10. Accumulation and ablation surfaces in 1955 and 2007..... 43
Figure 3. 11. Accumulation and ablation zones in LLGM paleo-glaciers..... 44